AIChE

Optimal Design and Planning of Sustainable Chemical Supply Chains Under Uncertainty

Gonzalo Guillén-Gosálbez
Dept. of Chemical Engineering, University Rovira i Virgili, Tarragona E-43007, Spain

Ignacio E. Grossmann
Dept. of Chemical Engineering, Carnegie Mellon University, Pittsburgh, PA 15213

DOI 10.1002/aic.11662
Published online November 11, 2008 in Wiley InterScience (www.interscience.wiley.com).

This article addresses the design of sustainable chemical supply chains in the presence of uncertainty in the life cycle inventory associated with the network operation. The design task is mathematically formulated as a bi-criterion stochastic mixed-integer nonlinear program (MINLP) that simultaneously accounts for the maximization of the net present value and the minimization of the environmental impact for a given probability level. The environmental performance is measured through the Eco-indicator 99, which incorporates the recent advances made in Life Cycle Assessment. The stochastic model is converted into its deterministic equivalent by reformulating the probabilistic constraint required to calculate the environmental impact in the space of uncertain parameters. The resulting deterministic bi-criterion MINLP problem is further reformulated as a parametric MINLP, which is solved by decomposing it into two sub-problems and iterating between them. The capabilities of the proposed model and solution procedure are illustrated through two case studies for which the set of Pareto optimal, or efficient solutions that trade-off environmental impact and profit, are calculated. These solutions provide valuable insights into the design problem and are intended to guide the decision maker towards the adoption of more sustainable design alternatives.
 AIChE J, 55: 99–121, 2009
Keywords: supply chain management, optimization, sustainability, uncertainty, life cycle assessment

Introduction

Traditionally, the optimization models devised in Process Systems Engineering (PSE) to assist in the operation and design of chemical processes have focused at the plant level. However, in the past decade, significant research effort has been devoted to extend the boundaries of the analysis to capture a broader range of business practices. This trend has been mainly motivated by the opportunity of achieving higher benefits through an integrated management of the whole supply chain (SC), and has been helped by advances in optimization theory and software applications. As a result of this trend, the area of supply chain management (SCM) has recently become a key issue in the chemical process industry and is expected to gain more importance in the future global market, in which the fierce competition will force companies to operate under tighter profit margins.

This paradigm shift in the scope of the analysis carried out in PSE has led to the development of a new generation of tools that provide decision-support for SCM.[1–7] These strategies enable the coordination and simultaneous optimization of manufacturing sites, logistics, and distribution tasks

Correspondence concerning this article should be addressed to I. E. Grossmann at grossmann@andrew.cmu.edu.

in a SC environment. The final aim is to find an overall optimal solution for the whole network in terms of some predefined criteria. This solution should not only optimize a given performance indicator, but also satisfy the set of mass balances, assignment, and capacity constraints imposed by the network topology.

The definition of an appropriate performance measure for the accurate and efficient assessment of the network operation poses a significant challenge that must be addressed when devising new modeling systems and solution techniques for SCM. In practice, the production–distribution activities undertaken by a firm are usually evaluated in terms of their ability to markedly improve the overall earnings of the company. For this reason, the economic benefit of the process has been traditionally pursued as the objective in the optimization procedure, and has become the most widely used performance indicator.[8] However, the decisions made by the firm in the context of SCM are not only driven by economic criteria. In fact, companies operate their SCs bearing in mind different conflicting goals related to diverse aspects of the business. These include, among many others, customer responsiveness,[9,10] flexibility,[11,12] and risk management.[13,14]

In particular, in the past years there has been a growing awareness of the importance of incorporating environmental concerns along with traditional economic criteria in the optimization of chemical processes. This trend has been motivated by several issues, a major one being the tighter governments regulations. In addition, the need to improve the customers' perception of the firm by being more environmentally conscious, which may eventually lead to higher product sales, has also contributed to this business trend.

The interest in incorporating pollution prevention techniques into process design is not new and dates back to the 1970s. Since then, numerous approaches have been proposed in the literature to decrease the energy and resource consumption in chemical plants (for a detailed review see Cano and McRae[15]). The main drawback of these strategies is that they usually focus on manufacturing, and therefore their scope is somewhat limited. Furthermore, they can sometimes lead to solutions that decrease the impact locally at the expense of increasing the negative effects in other stages of the life cycle of the product, in such a manner that the overall environmental damage is increased. To overcome this drawback, the boundaries of the study must be extended beyond the production stage to embrace a wider range of logistic activities. Thus, in the past decade it has become clear that the environmental issues must be considered throughout the entire production chain.

The field of Green supply chain management (GrSCM)[16] arose in response to this situation. This area addresses the influence and relationships between SCM and the natural environment. GrSCM has recognized the role played by SCM in sustainability and the possibility of taking advantage of this framework for holistically assessing the environmental performance of a process. Particularly, the application of SCM in this context is motivated by the system analysis that it adopts, which covers all the stages of the life cycle of the product. Regarding the PSE community, it is worth noting that the contribution made to GrSCM has been rather limited. Thus, although there are some articles in the field,[17–21] the area is still ripe for further research.

An extensive review with more than 227 citations related to GrSCM can be found in the work of Srivastava.[16] The author points out that mathematical programming (i.e., LP, NLP, MILP, and MINLP) has not been used extensively in the design of environmentally conscious SCs. Thus, although the potential benefits of such tools have been already acknowledged in the literature, little research has been conducted to date in this direction.

The use of mathematical programming in GrSCM offers the possibility of performing a simultaneous optimization of process operations and environmental issues. Unfortunately, the application of these techniques is hampered by the numerical difficulties that may arise when dealing with large scale problems. Furthermore, the environmentally conscious chemical process design problem is further complicated by the high degree of uncertainty brought about by external (demand, prices, costs, etc.) as well as internal factors (product yields, energy consumption, life cycle inventory, damage impact model, etc.).

Despite the importance of explicitly incorporating the treatment of uncertainties into the problem formulation, almost all the approaches devised to date in the area of sustainable chemical process design are deterministic.[17,21–25] These strategies assume nominal parameters values and do not provide any control on the variability of the environmental objective function over the different possible outcomes of the input parameters. This assumption has the disadvantage of leading to "optimistic" solutions that are optimal for the mean scenario, but have high probabilities of exceeding the nominal environmental performance.[26]

The aim of this article is to contribute to the emerging area of GrSCM by incorporating environmental concerns at the strategic level of SCM. Specifically, this work addresses the optimal design and planning of sustainable chemical processes and provides a quantitative tool based on mathematical programming that aims at facilitating the decision-making in this area. The main contribution of this article compared with other approaches devised to date is the explicit consideration of the uncertainty of the emissions released and feedstock requirements associated with the network operation. Furthermore, a novel decomposition technique is also provided to reduce the computational burden of the method and enhance its implementation in real industrial scenarios.

The overall problem is formulated as a bi-criterion stochastic mixed-integer nonlinear program (MINLP) that accounts for the maximization of the net present value (NPV) and minimization of the environmental impact for a given probability level. The identification of the Pareto optimal solutions of the resulting multi-objective MINLP is formulated as a parametric programming problem, which is solved by decomposing it into two hierarchical levels and iterating between them.

The article is organized as follows. A formal definition of the problem of interest is first presented. The mathematical model derived to address the problem under study is next given. The solution procedure proposed for the calculation of the Pareto optimal set is described in the following section,

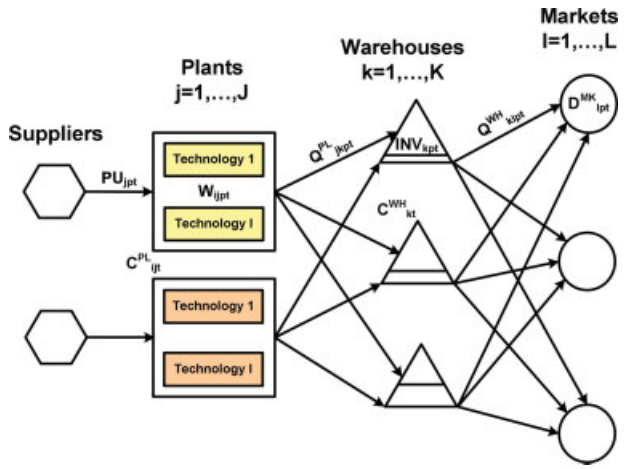

Figure 1. SC topology taken as reference.

[Color figure can be viewed in the online issue, which is available at www.interscience.wiley.com.]

and its performance is illustrated through two examples. Finally, some conclusions about this work are drawn.

Problem Statement

The SC design problem addressed in this article has as objective to determine the configuration of a three-echelon SC (production–storage–market) with the goal at maximizing the NPV and minimizing the environmental impact. Decisions to be made include the technologies installed in the plants, the capacity and location of the plants, and warehouses. The production rates and the material flows between the selected nodes of the SC. The structure of the three-echelon SC taken as reference in this work is depicted in Figure 1. This network includes the following elements:

- A set of plants with a set of available technologies, where products are manufactured.
- A set of warehouses where products are stored before being shipped to the markets.
- A set of markets where products are available to customers.

The environmentally conscious SC design can therefore be stated as follows.

Given are a fixed time horizon, demand and prices of products in each market and time period, fixed and variable investment costs associated with capacity expansions of plants and warehouses, fixed investment cost for the establishment of transportation links, lower and upper bounds on capacity expansions of plants and warehouses, costs associated with the SC operation (operating, raw materials, and inventory costs), interest rate, tax rate, and salvage value.

The goal is to determine the SC configuration along with the planning decisions that maximize the NPV and minimize the environmental impact. The decisions to be made include:

- Structural decisions: number, location and capacities of plants (including the technologies selected in each of them) and warehouses to be set; transportation links between the SC entities.
- Planning decisions: production rates at the plants in each time period; materials flows between plants, warehouses and markets, and sales of products.

The mathematical formulation is presented in the following section.

Mathematical Formulation

The most common approach to address the SC design problem is to formulate a large-scale mixed-integer program (MIP) that captures the relevant features associated with the network.[2,14,21,27] In this article a MIP is also proposed to address the environmentally conscious SC design. In a similar way as was done by Hugo and Pistikopoulos,[21] our model incorporates elements of the classical plant location problem[28] and the long range planning of chemical processes[29] within a single mathematical formulation. We should note that although the proposed model is based on the three-echelon SC previously described, it could easily be extended to more complex topologies. The equations involved in such a formulation are classified into three main groups. These are the mass balance equations, the capacity constraints, and the objective function. These sets of equations are described in detail in the next sections.

Mass balances

The mass balance must be satisfied in each of the nodes embedded in the network. Thus, for each plant j and chemical p, the purchases plus the amount produced must equal the amount transported from the plant to the warehouses plus the amount consumed.

$$\mathrm{PU}_{jpt} + \sum_{i \in \mathrm{OUT}(p)} \mathrm{W}_{ijpt} = \sum_{k} \mathrm{Q}^{\mathrm{PL}}_{jkpt} + \sum_{\mathrm{i} \in \mathrm{IN}(p)} \mathrm{W}_{ijpt} \quad \forall j,p,t \quad (1)$$

In Eq. 1, PU_{jpt} denotes the amount of product p purchased by plant j in time period t, W_{ijpt} is the input/output flow of p associated with technology i at plant j in t and $\mathrm{Q}^{\mathrm{PL}}_{jkpt}$ represents the amount of p transported between plant j and warehouse k in time period t. Regarding the purchases of products, let us note that these can be either raw materials or final products (i.e., outsourcing). For each product, the total purchases are constrained within lower ($\underline{\mathrm{PU}_{jpt}}$) and upper limits ($\overline{\mathrm{PU}_{jpt}}$), which are given by its availability in the current market place:

$$\underline{\mathrm{PU}_{jpt}} \le \mathrm{PU}_{jpt} \le \overline{\mathrm{PU}_{jpt}} \quad \forall j,p,t \quad (2)$$

Equation 3 is added to represent the material balance for each technology i installed at plant j.

$$\mathrm{W}_{ijpt} = \mu_{ip} \mathrm{W}_{ijp't} \quad \forall i,j,p,t \quad \forall p' \in \mathrm{MP}(i) \quad (3)$$

In this equation, μ_{ip} denotes the material balance coefficient for technology i and chemical p, whereas MP(i) is the set of main products corresponding to each technology.

Equation 4 represents the mass balance for the warehouses. Here, the initial inventory (INV_{kpt-1}) plus the amount transported from the plants j to the warehouse k must equal the material flow from the warehouse to the markets ($\mathrm{Q}^{\mathrm{WH}}_{klpt}$) plus the final inventory.

$$\mathrm{INV}_{kpt-1} + \sum_j \mathrm{Q}^{\mathrm{PL}}_{jkpt} = \sum_l \mathrm{Q}^{\mathrm{WH}}_{klpt} + \mathrm{INV}_{kpt} \quad \forall k,p,t \tag{4}$$

The sales of products at the markets (SA_{lpt}) are determined from the amount of materials sent by the warehouses, as it is stated in Eq. 5:

$$\sum_k \mathrm{Q}^{\mathrm{WH}}_{klpt} = \mathrm{SA}_{lpt} \quad \forall l,p,t \tag{5}$$

Finally, constraint 6 forces the total sales of product p at market l in period t to be greater than the minimum demand target level (i.e., the minimum demand that the firm wants to fulfill) ($\underline{\mathrm{D}^{\mathrm{MK}}_{lpt}}$) and lower than the maximum demand ($\overline{\mathrm{D}^{\mathrm{MK}}_{lpt}}$).

$$\underline{\mathrm{D}^{\mathrm{MK}}_{lpt}} \le \mathrm{SA}_{lpt} \le \overline{\mathrm{D}^{\mathrm{MK}}_{lpt}} \quad \forall l,p,t \tag{6}$$

Thus, the model assumes that part of the demand can be left unsatisfied because of limited production capacity or low product profitability.

Capacity Constraints

Plants. The capacity of each technology i at plant j in period t is represented by a continuous variable denoted by $\mathrm{C}^{\mathrm{PL}}_{ijt}$. Equation 7 constraints the production rate of technology i to be lower than the existing capacity and higher than a minimum desired percentage, τ, of the available installed capacity:

$$\tau \mathrm{C}^{\mathrm{PL}}_{ijt} \le \mathrm{W}_{ijpt} \le \mathrm{C}^{\mathrm{PL}}_{ijt} \quad \forall i,j,t \quad \forall p \in \mathrm{MP}(i) \tag{7}$$

The capacity of plant j in any time period t is calculated from the existing capacity at the end of the previous period plus the expansion in capacity carried out in t:

$$\mathrm{C}^{\mathrm{PL}}_{ijt} = \mathrm{C}^{\mathrm{PL}}_{ijt-1} + \mathrm{CE}^{\mathrm{PL}}_{ijt} \quad \forall i,j,t \tag{8}$$

In this equation, $\mathrm{CE}^{\mathrm{PL}}_{ijt}$ represents the expansion in capacity of technology i executed in period t at plant j.

Equation 9 is applied to bound the capacity expansions within lower and upper limits, which are denoted by $\underline{\mathrm{CE}^{\mathrm{PL}}_{ijt}}$ and $\overline{\mathrm{CE}^{\mathrm{PL}}_{ijt}}$, respectively.

$$\underline{\mathrm{CE}^{\mathrm{PL}}_{ijt}} X^{\mathrm{PL}}_{ijt} \le \mathrm{CE}^{\mathrm{PL}}_{ijt} \le \overline{\mathrm{CE}^{\mathrm{PL}}_{ijt}} X^{\mathrm{PL}}_{ijt} \quad \forall i,j,t \tag{9}$$

This equation makes use of the binary variable X^{PL}_{ijt}, which indicates the occurrence of the capacity expansion. This variable takes the value of 1 if technology i at plant j is expanded in capacity in time period t, and 0 otherwise.

Equation 10 limits the number of expansions for technology i available at plant j over the entire planning horizon.

$$\sum_t X^{\mathrm{PL}}_{ijt} \le \mathrm{nexp}^{\mathrm{PL}}_{ij} \quad \forall i,j \tag{10}$$

Note that the model presented assumes that a capacity expansion must start and end within a time period. In a design problem like the one addressed in our work, a time period has a length of one to several years. The decision-maker should then formulate the problem in such a way that the execution of the maximum allowable capacity expansion could always fit within one period.

Warehouses. The capacity of the warehouses is also represented by a continuous variable denoted by $\mathrm{C}^{\mathrm{WH}}_{kt}$. Equation 11 forces the total inventory kept at warehouse k to be lower than the available capacity in every time period t.

$$\sum_p \mathrm{INV}_{kpt} \le \mathrm{C}^{\mathrm{WH}}_{kt} \quad \forall k,t \tag{11}$$

Furthermore, the amount of products sent from a warehouse to the markets is constrained by its capacity. Thus, our model assumes that the capacity required to handle a given amount of products, assuming regular shipment and delivery schedule, is twice the average storage inventory level kept at the warehouse, which is denoted by IL_{kt}[30]:

$$2\mathrm{IL}_{kt} \le \mathrm{C}^{\mathrm{WH}}_{kt} \quad \forall k,t \tag{12}$$

The value of IL_{kt} is calculated from the output flow of materials and the turnover ratio of the warehouse ($\mathrm{tor_k}$), which represents the number of times that the stock is completely replaced per time period:

$$\mathrm{IL}_{kt} = \frac{\sum_l \sum_p \mathrm{Q}^{\mathrm{WH}}_{klpt}}{\mathrm{tor}_k} \quad \forall k,t \tag{13}$$

Finally, the capacity of the warehouse at any time period is determined from the previous one and the expansion in capacity executed in the same period:

$$\mathrm{C}^{\mathrm{WH}}_{kt} = \mathrm{C}^{\mathrm{WH}}_{kt-1} + \mathrm{CE}^{\mathrm{WH}}_{kt} \quad \forall k,t \tag{14}$$

Similarly, as with the plants, the value of $\mathrm{CE}^{\mathrm{WH}}_{kt}$ is bounded within lower and upper limits, as it is stated in Eq. 15.

$$\underline{\mathrm{CE}^{\mathrm{WH}}_{kt}} X^{\mathrm{WH}}_{kt} \le \mathrm{CE}^{\mathrm{WH}}_{kt} \le \overline{\mathrm{CE}^{\mathrm{WH}}_{kt}} X^{\mathrm{WH}}_{kt} \quad \forall k,t \tag{15}$$

This constraint includes the binary variable X^{WH}_{kt}, which equals 1 if an expansion in the capacity of warehouse k takes place in time period t and 0 otherwise.

Equation 16 limits the number of expansions of warehouse k over the entire planning horizon:

$$\sum_t X^{\mathrm{WH}}_{kt} \le \mathrm{nexp}^{\mathrm{WH}}_{k} \quad \forall k \tag{16}$$

Transportation Links. The existence of a transportation link between any two adjacent nodes of the network is represented by the binary variables $\mathrm{Y}^{\mathrm{PL}}_{jkt}$ and $\mathrm{Y}^{\mathrm{WH}}_{klt}$. A zero value of these variables prevents the flow of materials ($\mathrm{Q}^{\mathrm{PL}}_{jkpt}$ and $\mathrm{Q}^{\mathrm{WH}}_{klpt}$) between the corresponding nodes (i.e., between plant j and warehouse k and warehouse k and market l, respectively) from taking place in period t. On the other hand, a value of 1 allows the material flows within some lower and upper limits. The definition of these binary variables is enforced via the following constraints:

$$\underline{\mathrm{Q}^{\mathrm{PL}}_{jkt}} \mathrm{Y}^{\mathrm{PL}}_{jkt} \le \mathrm{Q}^{\mathrm{PL}}_{jkt} \le \overline{\mathrm{Q}^{\mathrm{PL}}_{jkt}} \mathrm{Y}^{\mathrm{PL}}_{jkt} \quad \forall j,k,p,t \tag{17}$$

$$\underline{\mathrm{Q}^{\mathrm{WH}}_{klt}} \mathrm{Y}^{\mathrm{WH}}_{klt} \le \mathrm{Q}^{\mathrm{WH}}_{klt} \le \overline{\mathrm{Q}^{\mathrm{EH}}_{klt}} \mathrm{Y}^{\mathrm{WH}}_{klt} \quad \forall k,l,p,t \tag{18}$$

Objective function

The SC design model previously described must attain two different targets. The economic objective is represented by the NPV, whereas the environmental concerns are measured by the Eco-indicator 99. The calculation of each of these metrics is described in detail in the next sections.

NPV. The NPV is calculated as the summation of the discounted cash flows generated in each of the time periods in which the total time horizon is divided (CF_t):

$$\mathrm{NPV} = \sum_t \frac{\mathrm{CF}_t}{(1+ir)^{t-1}} \tag{19}$$

In this equation, *ir* represents the interest rate. The cash flow in each time period is computed from the net earnings (i.e., profit after taxes), and the fraction of the total depreciable capital ($FTDC_t$) that corresponds to the period:

$$\mathrm{CF}_t = \mathrm{NE}_t - \mathrm{FTDC}_t \quad t = 1, \ldots, \mathrm{NT}-1 \tag{20}$$

Furthermore, in the calculation of the cash flow of the last time period ($t = NT$), it is necessary to take into account the fact that part of the total fixed capital investment (FCI) may be recovered at the end of the time horizon. This amount, which represents the salvage value of the network (sv), may vary from one type of industry to another.

$$\mathrm{CF}_t = \mathrm{NE}_t - \mathrm{FTDC}_t + \mathrm{svFCI} \quad t = \mathrm{NT} \tag{21}$$

The net earnings are given by the difference between the incomes and the total cost, as it is stated in Eq. 22. Here, revenues are determined from sales of final products, whereas the total cost includes (1) the purchases of raw materials, (2) the operating and inventory costs associated with plants and warehouses and (3) the cost of transporting materials between the SC entities.

$$\mathrm{NE}_t = (1-\varphi)\left[\sum_l \sum_p \gamma^{\mathrm{FP}}_{lpt}\mathrm{SA}_{lpt} - \sum_j \sum_p \gamma^{\mathrm{RM}}_{jpt}\mathrm{PU}_{jpt} - \sum_i \sum_j \sum_{p\in \mathrm{MP}(i)} \upsilon_{ijpt}\mathrm{W}_{ijpt} - \sum_k \pi_{kt}\mathrm{IL}_{kt} - \sum_j \sum_k \sum_p \psi^{\mathrm{PL}}_{jkpt}\mathrm{Q}^{\mathrm{PL}}_{jkpt} - \sum_k \sum_l \sum_p \psi^{\mathrm{WH}}_{klpt}\mathrm{Q}^{\mathrm{WH}}_{klpt}\right] + \varphi\mathrm{DEP}_t \quad \forall t \tag{22}$$

In this equation, φ denotes the tax rate, whereas $\gamma^{\mathrm{FP}}_{lpt}$ and $\gamma^{\mathrm{RM}}_{jpt}$ are the prices of final products and raw materials, respectively. Furthermore, υ_{ijpt} denotes the production cost per unit of main product *p* manufactured with technology *i* at plant *j* in period *t*, π_{kt} represents the inventory cost per unit of product stored in warehouse *k* during period *t*, and $\psi^{\mathrm{PL}}_{jkpt}$ and $\psi^{\mathrm{WH}}_{klpt}$ are the unitary transport costs. With regard to the depreciation of the capital invested, we will assume the straight-line method:

$$\mathrm{DEP}_t = \frac{(1-sv)\mathrm{FCI}}{\mathrm{NT}} \quad \forall t \tag{23}$$

where FCI denotes the total fixed cost investment, which is determined from the capacity expansions made in plants and warehouses as well as the establishment of transportation links during the entire time horizon as follows:

$$\mathrm{FCI} = \sum_i \sum_j \sum_t \left(\alpha^{\mathrm{PL}}_{ijt}\mathrm{CE}^{\mathrm{PL}}_{ijt} + \beta^{\mathrm{PL}}_{ijt}X^{\mathrm{P}}_{ijt}\right) + \sum_k \sum_t \left(\alpha^{WH}_{kt}CE^{WH}_{kt} + \beta^{WH}_{kt}X^{WH}_{kt}\right) + \sum_j \sum_k \sum_t \left(\beta^{TPL}_{jkt}Y^{PL}_{jkt}\right) + \sum_k \sum_l \sum_t \left(\beta^{\mathrm{TWH}}_{klt}\mathrm{Y}^{\mathrm{WH}}_{klt}\right) \tag{24}$$

Here, the parameters $\alpha^{\mathrm{PL}}_{ijt}$, $\beta^{\mathrm{PL}}_{ijt}$ and $\alpha^{\mathrm{WH}}_{kt}$, β^{WH}_{kt} are the variable and fixed investment terms corresponding to plants and warehouses, respectively. On the other hand, $\beta^{\mathrm{TPL}}_{jkt}$ and $\beta^{\mathrm{TWH}}_{klt}$ are the fixed investment terms associated with the establishment of transportation links between plants and warehouses, and warehouses and markets, respectively. Note that Eq. 24 reflects the concept of economies of scale. The total amount of capital investment can be constrained to be lower than an upper limit, as stated in Eq. 25

$$\mathrm{FCI} \le \overline{\mathrm{FCI}} \tag{25}$$

Finally, the model assumes that the payment of the fixed capital investment is divided into equal sums for each time period. Thus, the Fraction of Total Depreciable Capital ($FTDC_t$) is calculated as follows:

$$\mathrm{FTDC}_t = \frac{\mathrm{FCI}}{\mathrm{NT}} \quad \forall t \tag{26}$$

Environmental Impact Assessment: Application of LCA Principles. A key issue in the proposed methodology is how to evaluate the design alternatives from an environmental perspective. Defining a suitable environmental performance measure for the SC operation is not an easy task. In fact, so far there has not been an agreement about the index that should support objective environmental assessments, and it is very likely that such an agreement will never be reached.[15]

Specifically, this work makes use of the Eco-indicator 99[31] to assess the environmental performance of the network. This metric is based on the principles of Life Cycle Assessment (LCA). LCA is a methodology for evaluating the environmental loads associated with a product, process, or activity.[32] During its application, the energy and materials used in a process are first identified and quantified along with the waste released to the environment. This information is further translated into a set of environmental impacts that can be aggregated into different groups. These impacts are finally used to assess diverse process alternatives that may be implemented to achieve environmental improvements. Today, LCA has become the main instrument to evaluate the environmental performance of chemical processes.[21,23,33–35]

One of the main advantages of LCA is that it covers the entire life cycle of the product, process, or activity. This is achieved by expanding the boundaries of the study in order to include the upstream and downstream activities related to the main process itself. Thus, the essence of LCA is that it considers all material and energy flows from the "cradle" of primary resources (such as oil or ore deposits) to the "grave" of final disposal (such as stable inert material in a landfill). Furthermore, another advantage of LCA is that it employs a

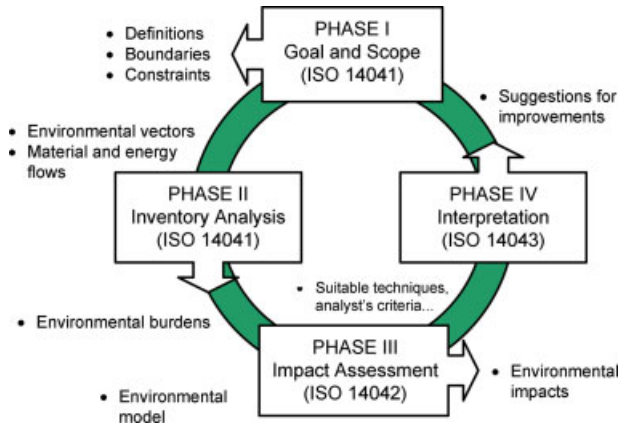

Figure 2. Phases of LCA.

[Color figure can be viewed in the online issue, which is available at www.interscience.wiley.com.]

damage model that links the emissions released and waste generated with the corresponding environmental damage. The calculation of the Eco-indicator 99 follows the four main LCA phases (see Figure 2). These are the goal and scope definition, the inventory analysis, the impact assessment, and the interpretation. Such phases are described in detail in the next sections.

Goal and scope definition. In this phase, the system boundaries and the impact categories are identified. Ideally, the boundaries of the system should include the entire life cycle of the process. However, in our specific case, the environmental analysis is restricted to the domain of SCM. Thus, we perform a "cradle-to-gate" analysis that embraces all the logistic activities from the extraction of raw materials to the delivery of final products to customers. However, this study does not include the associated downstream processes, such as secondary processing, product-use and disposal.

With regard to the impact categories, the Eco-indicator 99 accounts for the following 11 impact categories:

1. Carcinogenic effects on humans.
2. Respiratory effects on humans caused by organic substances.
3. Respiratory effects on humans caused by inorganic substances.
4. Damage to human health caused by climate change.
5. Human health effects caused by ionizing radiations.
6. Human health effects caused by ozone layer depletion.
7. Damage to ecosystem quality caused by ecosystem toxic emissions.
8. Damage to ecosystem quality caused by the combined effect of acidification and eutrophication.
9. Damage to ecosystem quality caused by land occupation and land conversion.
10. Damage to resources caused by extraction of minerals.
11. Damage to resources caused by extraction of fossil fuels.

These groups can be further aggregated into three damage categories: human health, ecosystem quality and resources. With regard to the functional unit of the analysis, this is defined as the total demand to be satisfied in the final markets over the entire time horizon.

Inventory analysis. The second phase provides the inputs and outputs of materials and energy associated with the process (Life Cycle Inventory), which are required to calculate the impacts in the different damage categories.

In the context of SCM, the environmental burdens are given by the production of raw materials and final products, the generation of the utilities consumed by the SC entities, and the transport of materials between them. In practice, the environmental data of the main process under study is usually available, whereas the one associated with the suppliers need to be retrieved from specific databases that contain the inventories of emissions and feedstock requirements of a wide range of chemical processes found in Europe.[36–38]

Mathematically, the inventory of emissions released and feedstock requirements associated with the SC operation can be expressed as a function of some continuous decision variables of the model. Specifically, they can be calculated from the purchases of raw materials (PU_{jpt}), the production rates at the manufacturing plants (W_{ijpt}) and the transport flows (Q^{PL}_{jkpt} and Q^{WH}_{klpt}), as stated in Eq. 27.

$$\begin{aligned} LCI_b = &\sum_j \sum_p \sum_t \omega^{PU}_{bp} PU_{jpt} + \sum_i \sum_j \sum_{p\in MP(i)} \sum_t \omega^{PR}_{bp} W_{ijpt} \\ &+ \sum_i \sum_j \sum_{p\in MP(i)} \sum_t \omega^{EN}_{b} \eta^{EN}_{ijp} W_{ijpt} \\ &+ \sum_j \sum_k \sum_p \sum_t \omega^{TR}_{b} \lambda^{PL}_{jk} Q^{PL}_{jkpt} \\ &+ \sum_k \sum_l \sum_p \sum_t \omega^{TR}_{b} \lambda^{WH}_{kl} Q^{WH}_{klpt} \quad \forall b \end{aligned} \tag{27}$$

In this equation, ω^{PU}_{bp}, ω^{PR}_{bp}, ω^{EN}_{b}, ω^{TR}_{b} and ω^{TR}_{b} denote the life cycle inventory entries (i.e., emissions released or feedstock requirements) associated with chemical b per reference flow of activity. In the raw materials production as well as the production of intermediate and final products, the reference flow is one unit of product manufactured. In the energy generation, the reference flow is one unit of fuel oil. The reference flow for the transport of materials is one unit of mass transported one unit of distance. Here, η^{EN}_{ijp} represents the consumption of energy per unit of product p manufactured with technology i at plant j in time interval t. This includes utilities such as electricity, steam, fuel, and cooling water, which are converted into fuel oil equivalent tons (FOET). Thus, the life cycle inventory of the generation and supply of thermal energy from the combustion of one unit of fuel oil can be used to estimate the consumption of utilities. Finally, λ^{PL}_{jk} and λ^{WH}_{kl} denote the distance between plants and warehouses and warehouses and markets, respectively.

Note that to avoid double counting in the calculation of the life cycle inventory, ω^{PR}_{bp} should only include the direct emissions (i.e., fugitive emissions) of the main processes under study. Finally, let us mention that this equation can easily be modified to account for by-products and energy savings, if this was necessary.

Impact assessment. In this stage, the process data are translated into environmental information. As was mentioned before, three different damage categories are considered in the computation of the Eco-indicator 99. The human health damages are specified in Disability Adjusted Life Years (DALYs). A damage of 1 means that 1 life year of one individual is lost, or one person suffers 4 years from a disability with a weight of 0.25. On the other hand, the ecosystem quality damages are specified as PDF·m^2·year. PDF stands for Potentially Disap-

pear Fraction of Species. A damage of 1 means all species disappear from 1 m^2 during 1 year, or 10 % of all species disappear from 1 m^2 during 10 years. With regard to the damages to resources, these are specified as MJ surplus energy. A damage of 1 means that due to a certain extraction of resources, further extraction of the same resources in the future will require one additional MJ of energy due to the lower resource concentration or other unfavorable characteristics of the remaining reserves. The specific point in the future is chosen arbitrarily as the time at which five times the cumulative extraction of the resource before 1990 is extracted.[31]

The damage caused in each impact category c belonging to a specific damage category d (IM_c) is calculated from the life cycle inventory and the corresponding set of damage factors (θ_{bc}), as stated in Eq. 28.

$$IM_c = \sum_b \theta_{bc} LCI_b \quad \forall c \tag{28}$$

The damage factors are the link between the results of the inventory phase and the damage in each impact category. For instance, for the human health damage category, the corresponding damage model includes: (1) a fate analysis, to link any emission, which is expressed in terms of mass, to a temporary change in concentration; (2) an exposure analysis, to link this temporary concentration to a dose; (3) an effect analysis, to link the dose to a number of health effects; (4) a damage analysis to translate the health effects into DALYs.

Furthermore, there are three different damage models available in the Eco-indicator 99 framework according to three different perspectives based on Cultural Theory.[31] In the Egalitarian perspective, which is a long-term perspective, even a minimum of scientific proof justifies inclusion of effects. In the Individualist (short time perspective), only proven effects are included. In the Hierarchist (balanced time perspective), consensus among scientist determines inclusion of effects. The impact caused in each damage category can be finally calculated by using Eq. 29:

$$DAM_d = \sum_{c \in ID(d)} IM_c \quad \forall d \tag{29}$$

Here $ID(d)$ denotes the set of impact categories c that contribute to damage d. Finally, the damages are normalized and aggregated into a single impact factor (i.e., Eco-indicator 99), as stated in Eq. 30.

$$ECO_{99} = \sum_d \delta_d \xi_d \cdot DAM_d \tag{30}$$

This equation makes use of normalization (δ_d) and weighting (ξ_d) factors. The normalization set is based on a damage calculation of all relevant European emissions, extractions and land-uses. As there are three damage models, there are also three normalization sets. With regard to the weighing method, there are four versions of the weighting set: one average for all panelists, and three versions for subgroups of the panel, which could be regarded as adhering to a perspective. Specifically, this work applies the Hierarchist perspective combined with the default (average) weighting factors.

Interpretation. Finally, in the fourth phase the results are analyzed and a set of conclusions or recommendations for the system are formulated. In this regard, the final goal of LCA is to provide criteria and quantitative measures that may be used for comparing different process operation and design alternatives. One of the main shortcomings of LCA is that it lacks a systematic way of generating such alternatives and identify the best ones in terms of environmental performance. This drawback can be overcome by coupling LCA with optimization tools. Although the potential benefits of combining LCA and process optimization within a single framework have been already acknowledged in the literature, only a limited number of case studies have been reported to date.[21,23]

Notice that as opposed to other techniques that account for environmental concerns by adding constraints on operations, in our work the preferences are articulated in the post-optimal analysis of all the Pareto optimal solutions. This approach provides further insights into the design problem and allows for a better understanding of the inherent trade-off between economic and environmental criteria.

Uncertainty in the life cycle inventory. Many LCA studies assume nominal values for the input data and do not include a systematic way of assessing the validity of the environmental analysis in the space of uncertain parameters.[39] However, the Eco-indicator 99 methodology is affected by three main sources of uncertainty.[31] These are: (1) the operational or data uncertainty, (2) the fundamental or model uncertainties, and (3) the uncertainty on the completeness on the model. Whereas the second and third sources of uncertainty cannot be covered by standard statistical analysis, the first one can be easily documented. For this reason, our analysis is restricted to the operational uncertainties.

The operational uncertainties include the uncertainty associated with the inventory results (i.e., emissions released and feedstock requirements), and the one related to the damage model. The uncertainties that affect the damage assessment calculations are difficult to document and quantify.[31] For this reason, we consider that the damage factors of the damage model can be perfectly known in advance and focus on the uncertainty associated with the life cycle inventory. This source of uncertainty arises from the lack of reliable information regarding the emissions due to the operation of the systems that provide raw materials and utilities to the SC under study. We assume that the emissions released and resources consumed per unit of reference flow of activity follow Gaussian distributions whose mean values and standard deviations must be provided as input data by the decision-maker. This assumption makes it possible to perform an analytical integration of the probability function that characterizes the Eco-indicator 99. The normal probability distribution is one of the most widely used statistical distributions in LCA and has been repeatedly applied in the LCA literature.[39–41]

Usually stochastic optimization models attempt to account for uncertainty by optimizing the expected performance of the objective function. However, this strategy does not reflect the variability of performances in the space of uncertain parameters. Therefore, in this work we propose to control the variability of the environmental impact by accounting for the minimization of the Eco-indicator 99 for a given probability level. The definition of this performance measure gives rise to the following probabilistic constraint (see Figure 3):

$$\Pr[ECO_{99} \leq \Omega] \geq \kappa \tag{31}$$

Here, κ is the probability level that has to be defined beforehand, whereas Ω denotes the Eco-indicator 99 value

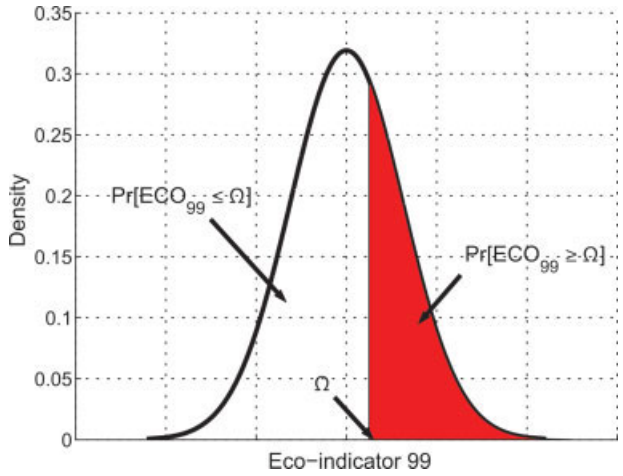

Figure 3. Probabilistic analysis of the environmental performance.

[Color figure can be viewed in the online issue, which is available at www.interscience.wiley.com.]

associated with that probability level. The value of Ω should then be appended to the objective function as an additional criterion to be optimized along with the NPV.

In Eq. 31, ECO_{99} is a random variable that is normally distributed due to the normality assumption associated with the life cycle inventory results per reference flow of activity (see Figure 3). The deterministic equivalent of this probabilistic constraint can be obtained by applying general concepts from chance constrained programming.[42–44] Specifically, by subtracting the mean ($\widehat{ECO}_{99}$) and dividing by the standard deviation of the Eco-indicator 99 (ECO_{99}^{SD}), the chance constraint can be written as:

$$\Pr\left[\frac{ECO_{99} - \widehat{ECO}_{99}}{ECO_{99}^{SD}} \leq \frac{\Omega - \widehat{ECO}_{99}}{ECO_{99}^{SD}}\right] \geq \kappa \tag{32}$$

If the uncertain parameters are assumed to follow independent uncorrelated normal distributions, then the mean and the standard deviation of the Eco-indicator 99 can be calculated as follows:

$$\begin{aligned}\widehat{ECO}_{99} = &\sum_b \sum_{c\in ID(d)} \sum_d \sum_j \sum_p \sum_t \delta_d \xi_d \theta_{bc} \hat{\omega}_{bp}^{PU} PU_{jpt} \\ &+ \sum_b \sum_{c\in ID(d)} \sum_d \sum_i \sum_j \sum_{p\in MP(i)} \sum_t \delta_d \xi_d \theta_{bc} \hat{\omega}_{bp}^{PR} W_{ijpt} \\ &+ \sum_b \sum_{c\in ID(d)} \sum_d \sum_i \sum_j \sum_{p\in MP(i)} \sum_t \delta_d \xi_d \theta_{bc} \hat{\omega}_{b}^{EN} \eta_{ijp}^{EN} W_{ijpt} \\ &+ \sum_b \sum_{c\in ID(d)} \sum_d \sum_j \sum_k \sum_p \sum_t \delta_d \xi_d \theta_{bc} \hat{\omega}_{b}^{TR} \lambda_{jk}^{PL} Q_{jkpt}^{PL} \\ &+ \sum_b \sum_{c\in ID(d)} \sum_d \sum_k \sum_l \sum_p \sum_t \delta_d \xi_d \theta_{bc} \hat{\omega}_{b}^{TR} \lambda_{kl}^{WH} Q_{klpt}^{WH}\end{aligned} \tag{33}$$

$$\begin{aligned}ECO_{99}^{SD} = &\sum_b \sum_{c\in ID(d)} \sum_d \sum_j \sum_p \sum_t (\delta_d \xi_d \theta_{bc} \sigma_{bp}^{PU} PU_{jpt})^2 \\ &+ \sum_b \sum_{c\in ID(d)} \sum_d \sum_i \sum_j \sum_{p\in MP(i)} \sum_t (\delta_d \xi_d \theta_{bc} \sigma_{bp}^{PR} W_{ijpt})^2 \\ &+ \sum_b \sum_{c\in ID(d)} \sum_d \sum_i \sum_j \sum_{p\in MP(i)} \sum_t (\delta_d \xi_d \theta_{bc} \sigma_{b}^{EN} \eta_{ijp}^{EN} W_{ijpt})^2 \\ &+ \sum_b \sum_{c\in ID(d)} \sum_d \sum_j \sum_k \sum_p \sum_t (\delta_d \xi_d \theta_{bc} \sigma_{b}^{TR} \lambda_{jk}^{PL} Q_{jkpt}^{PL})^2 \\ &+ \sum_b \sum_{c\in ID(d)} \sum_d \sum_k \sum_l \sum_p \sum_t (\delta_d \xi_d \theta_{bc} \sigma_{b}^{TR} \lambda_{kl}^{WH} Q_{klpt}^{WH})^2 \Big]^{1/2}\end{aligned} \tag{34}$$

In these equations, $\hat{\omega}_{bp}^{PU}$, $\hat{\omega}_{bp}^{PR}$, $\hat{\omega}_{b}^{EN}$, $\hat{\omega}_{b}^{TR}$ denote the mean of the life cycle inventory results per reference flow of activity, whereas σ_{bp}^{PU}, σ_{bp}^{PR}, σ_{b}^{EN}, and σ_{b}^{TR} are the standard deviations of the corresponding normal distributions. Note that the square root function that appears in constraint 34 is convex, as has been shown by Kataoka.[45]

The left hand side of the equality within the probabilistic sign of constraint 32 is now a normally distributed random variable with a mean value of 0 and a variance of 1 (standardized form). This allows us to replace the chance constraint by the following deterministic equivalent expression:

$$\Phi\left(\frac{\Omega - \widehat{ECO}_{99}}{ECO_{99}^{SD}}\right) \geq \kappa \tag{35}$$

where $\Phi(\cdot)$ denotes the standardized normal cumulative probability function. The inverse of this function, which is denoted by $\Phi^{-1}(\cdot)$, can be next applied to obtain the following expression:

$$\frac{\Omega - \widehat{ECO}_{99}}{ECO_{99}^{SD}} \geq \Phi^{-1}(\kappa) \tag{36}$$

which finally leads to:

$$ECO_{99}^{SD}\Phi^{-1}(\kappa) + \widehat{ECO}_{99} \leq \Omega \tag{37}$$

This equation can be combined with Eq. 33 and 34 in order to replace the values of $\widehat{ECO}_{99}$ and ECO_{99}^{SD} by their corresponding mathematical defintion. This gives rise to a nonlinear constraint, the convexity of which can be preserved for positive values of $\Phi^{-1}(\kappa)$.[45]

This transformation also allows to further reformulate the model as a parametric programming problem with an uncertain parameter in the right hand side of one constraint, as it will be discussed in the next section. Finally, the overall mathematical model can be written as follows:

$$\begin{array}{ll}\max & (NPV, -\Omega) \\ \text{s.t.} & \text{Eqs. 1–30, and 37}\end{array}$$

For the sake of simplicity, this model will be represented from now on as follows:

$$\begin{array}{lll}(M) & \max\limits_{x,y} & (NPV(x,y), -\Omega(x,y)) \\ & \text{s.t} & h(x,y) = 0 \\ & & g(x,y) \leq 0 \\ & & x \in \Re^n,\ y \in \{0.1\}^m\end{array}$$

where x and y denote the continuous and binary variables of the model, respectively. $h(x,y) = 0$ denote the equality constraints, which are all linear. The inequality constraints, which are represented by $g(x,y) \leq 0$, are all linear except the one that defines Ω (i.e., Eq. 37), which is nonlinear but convex.

Solution Procedure

For the calculation of the Pareto set of (M), two main methods exist in the literature. These are the weighted-sum method and the ε-constraint method.[46] Specifically, both of these methods are based on formulating a single-objective problem that is related to the original multi-objective one. This problem is then solved repeatedly for different values of some auxiliary parameters introduced in the model. In the weighted-sum method, which is only rigorous for the case of convex problems, these parameters take the form of a vector of weighs that multiplies the vector of objectives. In the ε-constraint method, which is also rigorous for the nonconvex case, they represent the limits imposed to those objectives of the multi-objective problem (MOP) that are transferred to some additional constraints. Each single-objective problem provides a weakly efficient point of the MOP. However, the strictly efficiency of such solutions can only be guaranteed after exploring the whole space of auxiliary parameters.

The identification of the noninferior solutions of (M) with the ε-constraint method can be formulated as a parametric programming problem of the following form:[47]

$$\begin{aligned} (\text{P1})\ \hat{z}(\varepsilon) = \max_{x,y}\ & \text{NPV}(x,y) \\ \text{s.t}\ & \Omega(x,y) \leq \varepsilon \\ & \underline{\varepsilon} \leq \varepsilon \leq \overline{\varepsilon} \\ & h(x,y) = 0 \\ & g(x,y) \leq 0 \\ & x \in \Re^n, y \in \{0,1\}^m \end{aligned}$$

where the lower and upper limits $\underline{\varepsilon}$ and $\overline{\varepsilon}$ that define the interval within which the ε parameter must fall are obtained from the optimization of each separate scalar objective:

$$\begin{aligned} (\text{P1a})\ (\bar{x},\bar{y}) = \arg\min_{x,y}\ & \Omega(x,y) \\ \text{s.t.}\ & h(x,y) = 0 \\ & g(x,y) \leq 0 \\ & x \in \Re^n, y \in \{0,1\}^m \end{aligned}$$

which defines $\underline{\varepsilon} = \Omega(\bar{x},\bar{y})$ and

$$\begin{aligned} (\text{P1}b)\ (\bar{x},\bar{y}) = \arg\max_{x,y}\ & \text{NPV}(x,y) \\ \text{s.t.}\ & h(x,y) = 0 \\ & g(x,y) \leq 0 \\ & x \in \Re^n, y \in \{0,1\}^m \end{aligned}$$

which defines $\overline{\varepsilon} = \Omega(\overline{x},\overline{y})$.

Problem (P1) can then be solved by algorithms based on parametric programming. These strategies determine the set of critical regions of the parametric problem and the associated parametric profiles.[47] The main advantage of parametric programming compared with standard scalarization techniques, is that it avoids the need of exhaustively enumerating the entire space of auxiliary parameters.

Proposed Decomposition Technique

The decomposition technique applied for solving (P1) is inspired on the work of Pertsinidis et al.,[48] which focused on solving bi-criterion MILPs. Our strategy is based on decomposing (P1) into two levels. In the upper level, a master convex MINLP, in which the ε parameter is treated as a free variable, is solved to provide a vector of integer variables. This vector is then passed to the lower level, in which a parametric NLP resulting from fixing the binary variables calculated by the upper level is solved to obtain a lower bound to problem (P1). This procedure is repeated iteratively. In each iteration, the master problem is forced to improve the current lower bound (i.e., the current approximation of the Pareto set) in at least one point, whereas the parametric profile is updated with the results of the new parametric NLP being solved.

From now on and without loss of generality, it will be assumed that the NPV is regarded as main objective and the environmental impact is transferred to the auxiliary epsilon constraint. The steps of the algorithm are described in detail in the following sections.

Initialization

This step requires the initialization of the parameters of the algorithm, mainly the iteration count, the lower bound and the set of best integer solutions. The lower and upper limits $\underline{\varepsilon}$ and $\overline{\varepsilon}$ within which the value of Ω must fall are also determined in this first step. The computation of $\overline{\varepsilon}$, which is obtained by solving (P1b), provides the first integer solution that will be taken as a basis for calculating future improvements. Let the solution of this problem be given by $y = \overline{y}$.

Lower level: Parametric NLP

Here, the solution $\overline{y}$ provided by the upper level is fixed in (P1), and the resulting parametric NLP is solved:

$$\begin{aligned} (\text{P2})\ \hat{z}(\varepsilon,\overline{y}) = \max_{x,\varepsilon}\ & \text{NPV}(x,\overline{y}) \\ \text{s.t}\ & \Omega(x,\overline{y}) \leq \varepsilon \\ & \underline{\varepsilon} \leq \varepsilon \leq \overline{\varepsilon} \\ & h(x,y) = 0 \\ & g(x,y) \leq 0 \\ & x =\in \Re^n, y \in \{0,1\}^m \end{aligned}$$

The solution of this problem can be obtained by performing a sensitivity analysis with respect to ε. Specifically, in this article we apply the method proposed by Fiacco[49] (see Appendix). The underlying idea consists of approximating the parametric NLP solution by a piecewise linear function that provides a valid lower bound to the true parametric solution of (P2) with a given tolerance error tol. This lower bound, denoted by $\widehat{z}(\varepsilon,\overline{y})$, comprises a set of linear intervals, labeled as $\widehat{z_n}(\varepsilon,\overline{y})$, that have the following form:

$$\widehat{z_n}(\varepsilon,\overline{y}) = a_n + b_n(\varepsilon - \varepsilon_n) \tag{38}$$

Furthermore, each of these linear intervals corresponds to a different critical region CR_n of (P2). The entire parametric

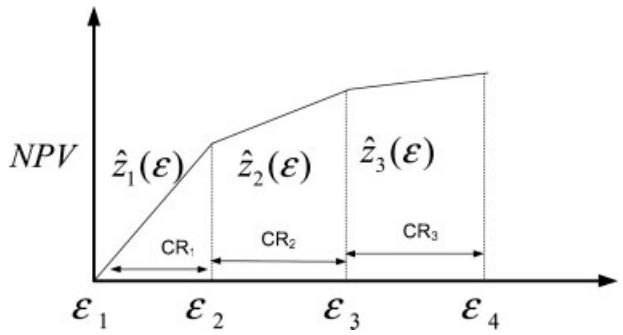

Figure 4. Solution of parametric NLPs.

profile $\hat{z}(\varepsilon,\overline{y})$ is a valid lower bound of (P2), and thus a valid lower bound of (P1). Figure 4 illustrates the parametric solution of an NLP, which comprises 3 critical regions. The parametric solution in critical region n, which corresponds to the interval$[\varepsilon_n,\varepsilon_{n+1}]$, is given by the linear profile $\hat{z_n}(\varepsilon,\overline{y})$.

Comparison of parametric profiles

The parametric profile associated with (P2) (i.e., $\hat{z}(\varepsilon,\overline{y})$) is intersected with the current lower bound (i.e., $\hat{z^*}(\varepsilon)$), so the latter can be updated. Note that in the first iteration of the algorithm the lower bound is set to $-\infty$, and therefore the comparison procedure reduces to making the lower bound equal to the current parametric NLP solution.

Figure 5 illustrates the comparison step that must be performed in further iterations of the algorithm. Specifically, the figure depicts the intersection between a parametric NLP solution and a possible current lower bound. The lower bound involves two different discrete solutions, which are denoted by $\overline{y^{*1}}$ and $\overline{y^{*2}}$, whereas the NLP profile is associated with solution $\overline{y}$. The set $\overline{\mathcal{Y}}^*$ includes all the discrete solutions that appear in the lower bound, in this case $\overline{\mathcal{Y}}^* := \{\overline{y^{*1}}, \overline{y^{*2}}\}$. The comparison between the profiles is carried out by keeping the best linear profile and discrete solution for each intersecting interval. Note that each profile may have a different number of critical regions that will overlap. As a result of this step, a new current lower bound with a new set of critical regions and integer solutions is obtained. Specifically, in this example, there are 4 critical regions and 2 different discrete solutions in the lower bound profile. The comparison step leads to an updated lower bound with 5 critical regions and 3 discrete solutions. These new linear intervals and discrete solutions, which represent the actual best approximation to the Pareto set, will be updated in the next iterations of the algorithm.

Upper level: Master MINLP

If the current lower bound $\hat{z^*}(\varepsilon)$ cannot be improved in the region $[\underline{\varepsilon},\overline{\varepsilon}]$, then it represents the Pareto set to the original MOP. However, the need of restructuring the SC according to the specific environmental restrictions to be met in each case will make this situation quite unusual. Thus, in general it will be possible to find a solution able to exceed the current lower bound in at least one point. To identify such a solution, it is necessary to unlock the binary variables and force the model to improve the current lower bound in at least one linear interval. Thus, the search of this new integer solution requires the definition of a customized convex MINLP of the following form:

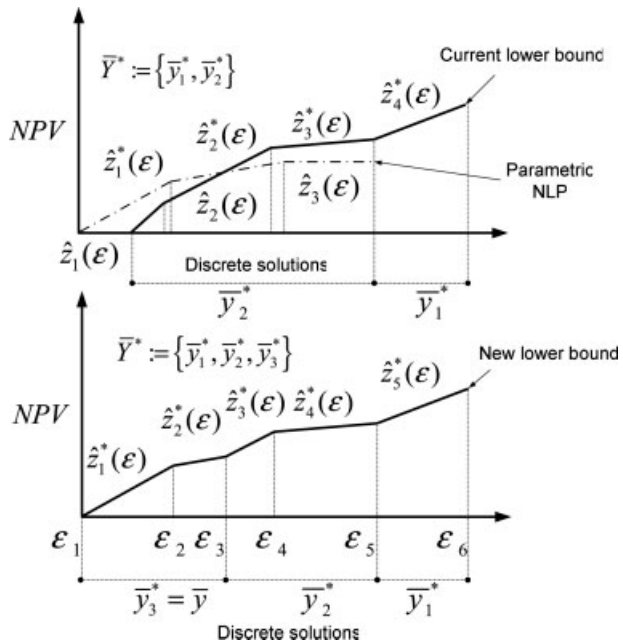

Figure 5. Comparison step.

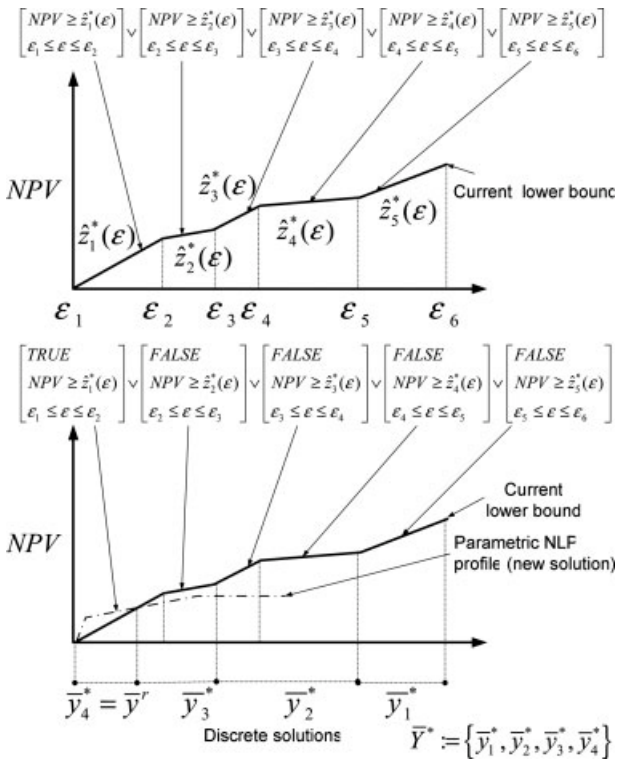

Figure 6. Master MINLP.

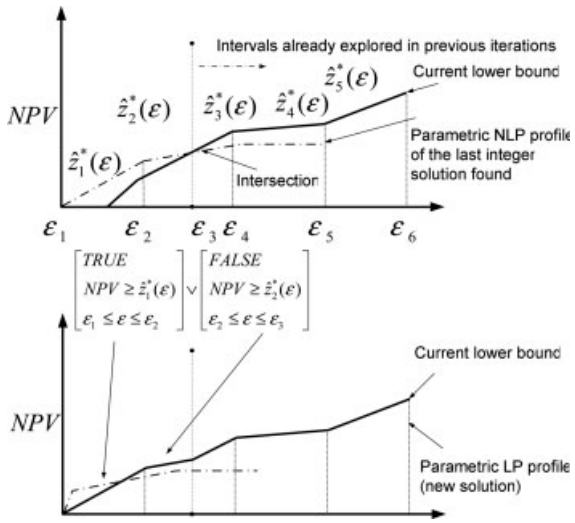

Figure 7. Disjunctive term of the master MINLP.

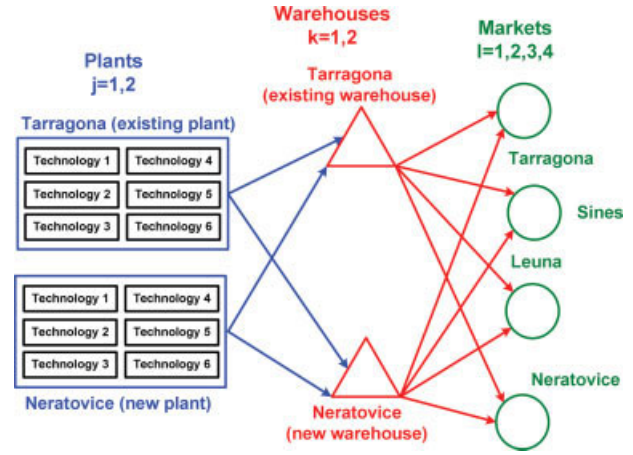

Figure 8. Case study 1.

[Color figure can be viewed in the online issue, which is available at www.interscience.wiley.com.]

$$\max_{x,y} \mathrm{NPV}(x,y) \quad (P3)$$

s.t.

$$\bigvee_{n}\begin{bmatrix}\mathrm{NPV}(x,y) \geq \hat{z} *_n (\varepsilon) + \mathrm{tol} \\ \varepsilon_n \leq \varepsilon \leq \varepsilon_{n+1}\end{bmatrix}$$

$$\sum_{m\in F_r^1} y_m^r - \sum_{m\in F_r^0} y_m^r \leq |F_r^1| - 1 \quad \forall r; F_r^1 := \{m|\bar{y}_m^r = 1\};$$

$$F_r^0 := \{m|\bar{y}_m^r = 0\};$$

$$h(x,y) = 0$$

$$g(x,y) \leq 0$$

$$x \in \Re^n, \varepsilon \in \Re^1, y \in \{0,1\}^m$$

This master MINLP is based on model (P1) but incorporates two additional elements. The first one is a parametric cut that takes the form of a disjunctive term and forces the model to find a solution that exceeds the current lower bound $\widehat{z^*}(\varepsilon)$. Notice that the exact interval in which the current solution will be exceeded by the new integer successor cannot be known in advance. For this reason, all the critical regions found so far must be included in the disjunction.

Specifically, among the possible integer solutions that satisfy the above requirement, the interest is placed on the one that first intersects the current lower bound profile. This allows the sequential generation of the whole family of integer solutions that appear in the Pareto set. The requirement of finding the first of the integer solutions that satisfy this

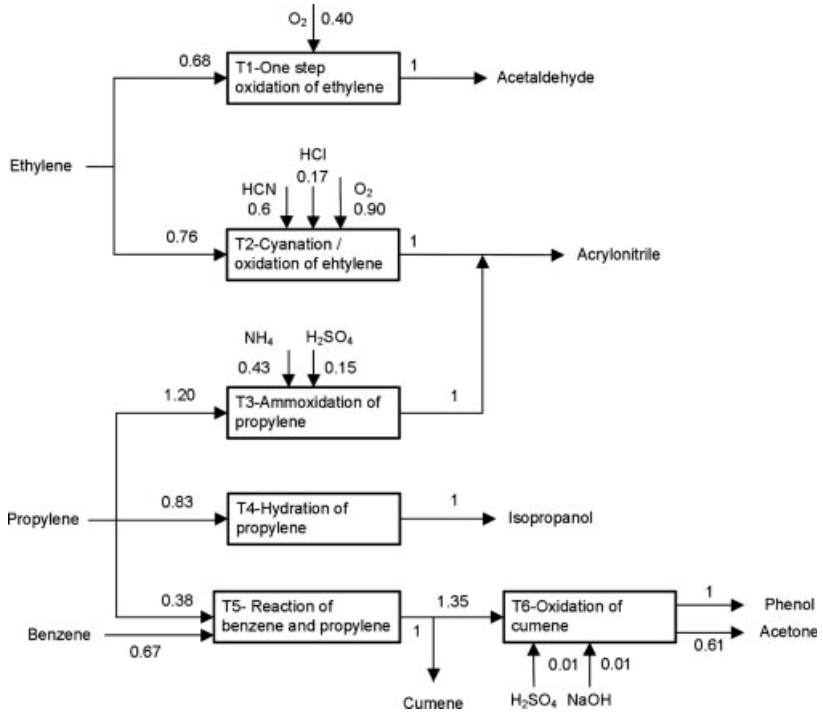

Figure 9. Superstructure of technologies of case study 1.

Table 1. Case Study 1: Variable and Fixed Investment Cost of Plants for t = 1 (assume a 5% increase in each period of time)

	α_{ijt}^{PL} ($·year/ton)		β_{ijt}^{PL} (thousand $)	
Tech./Plant	Neratovice	Tarragona	Neratovice	Tarragona
T1	91.28	109.53	8,306.45	9,967.74
T2	93.43	112.12	8,502.82	10,203.38
T3	235.81	282.97	21,459.49	2,5751.38
T4	104.73	125.68	9,530.80	1,1436.97
T5	46.34	55.60	4,216.72	5,060.06
T6	165.59	198.70	15,069.01	18,082.81

property is automatically fulfilled by keeping always the same objective function (i.e., the NPV). Thus, the proposed algorithm takes advantage of the monotonicity property of the Pareto curve and avoids having to explore each critical region separately, as the general purpose algorithms for parametric programming usually do.[50]

Figure 6 illustrates the way in which the master MINLP operates. The disjunction forces to improve the current lower bound in at least one of the intervals. In this case, the current lower bound is exceeded in its first linear interval. The solution found is then fixed in the parametric NLP to calculate a new parametric profile that must be intersected with the current lower bound. The figure also depicts the comparison between the parametric NLP profile of the new integer solution, denoted by y^{*4}, and the current lower bound. This step is repeated iteratively until the termination criteria is satisfied.

The second type of cuts in (P3) are integer cuts that are applied to exclude the solutions found so far. In this equation, F_r^0 and F_r^1 represent, for each previous iteration r, the sets of integer variables valued at one and zero respectively, and $|F_r^1|$ is the cardinality of the set F_r^1.

Note that if there is no feasible solution to the master MINLP (P3), the current lower bound represents the Pareto set. This situation arises when the lower bound cannot be improved. We should also note that (P3) can be converted into a standard convex MINLP by employing either the convex hull[51] or the big-M reformulation.[52]

Algorithmic steps

The steps of the algorithm are next summarized.

• **Step 0** (initialization). Set the following values: iteration count, $r = 0$; lower bound,$\widehat{z^*}(\varepsilon) = -\infty$; set of Pareto optimal integer solutions $\overline{\mathcal{Y}}^* := \{\emptyset\}$. Calculate the lower and upper limits $\underline{\varepsilon}$ and $\overline{\varepsilon}$ within which the value of Ω must fall. The computation of $\overline{\varepsilon}$, which is obtained by solving (P1b), provides in turn the first integer solution $\overline{y}$.

Table 2. Case Study 1: Operating Cost for t = 1 (assume a 5% increase in each period of time) and Consumption of Energy

	v_{ijpt} ($/ton)		η_{ijp}^{EN}
Tech./Plant	Neratovice	Tarragona	(FOET/ton)
T1	13.36	16.03	0.22
T2	36.42	43.71	0.60
T3	9.11	10.93	0.15
T4	23.07	27.68	0.38
T5	3.64	4.37	0.06
T6	23.07	27.68	0.38

Table 3. Case Study 1: Price of Final Products for $t = 1$ (assume a 5% increase in each period of time)

	γ_{ipt}^{FP} ($/ton)			
Chemical/Market	Leuna	Neratovice	Sines	Tarragona
Acetaldehyde	509.26	487.43	491.07	500.17
Acetone	432.87	414.32	417.41	425.14
Acrylonitrile	36.40	34.84	35.10	35.75
Cumene	401.23	384.04	386.90	394.07
Isopropanol	401.23	384.04	386.90	394.07
Phenol	709.88	679.45	684.52	697.20

• **Step 1** (parametric NLP). Solve the parametric NLP resulting from fixing $\overline{y}$ in (P1) (see Appendix) and obtain the corresponding parametric profile $\hat{z}(\varepsilon, \overline{y})$. Update the iteration count, $r = r + 1$.

• **Step 2** (comparison of parametric solutions). Compare $\widehat{z^*}(\varepsilon)$ with $\widehat{z}(\varepsilon, \overline{y})$. If $\widehat{z}(\varepsilon, \overline{y}) \geq \widehat{z^*}(\varepsilon)$ for some linear interval of ε, update the best current lower bound $\widehat{z^*}(\varepsilon)$ and the associated set of best integer solutions $\overline{\mathcal{Y}}^*$ with the values of $\widehat{z}(\varepsilon, \overline{y})$ and $\overline{y}$.

• **Step 3** (master subproblem). Formulate and solve the master MINLP (P3), treating ε as a free variable and introducing parametric cuts of the form NPV $\geq \widehat{z_n^*}(\varepsilon) + \text{tol}$, and integer cuts for excluding previous explored solutions. If (P3) is infeasible, stop; otherwise store the value of the integer solution found by (P3) (i.e., $\overline{y}$) and go to step 1.

Remarks

It is interesting to highlight the following aspects of the algorithm:

• The proposed decomposition strategy provides the Pareto set of (M) in a finite number of major iterations. The number of iterations is equal to the number of different integer solutions of the Pareto set plus one.

• The disjunction of (P3) must be constructed according to the current lower bound. Notice that it is not necessary to include in the disjunctive term the intervals beyond the intersection between the current lower bound and the NLP parametric profile of the last integer solution found, as these intervals were already explored in previous iterations. Figure 7 illustrates this idea. Specifically, it shows how the current lower bound depicted in Figure 6 cannot be improved in intervals beyond the intersection point, as these intervals were already evaluated by (P3) in previous runs. As men-

Table 4. Case Study 1: Cost of Raw Materials for t = 1 (assume a 5% increase in each period of time)

	γ_{jpt}^{RM}($/ton)	
Chemical/Plant	Neratovice	Tarragona
Ammonia	140.54	148.81
Benzene	200.51	212.30
Ethylene	233.68	247.42
Hydrochloric acid	116.18	123.02
Hydrogen cyanide	468.47	496.03
Oxygen	29.98	31.75
Propylene	159.28	168.65
Sodium hidroxide	140.54	148.81
Sulfuric acid	42.16	44.64

Table 5. Case Study 1: Demand of Products for $t = 1$ (assume a 5% increase in each period of time)

	$\overline{D_{lpt}^{MK}}$ (kton/year)			
Chemical/Market	Leuna	Neratovice	Sines	Tarragona
Acetaldehyde	13.5	37.5	12.0	7.5
Acetone	10.8	30.0	9.6	6.0
Acrylonitrile	18.0	50.0	16.0	10.0
Cumene	13.5	37.5	12.0	7.5
Isopropanol	9.0	25.0	8.0	5.0
Phenol	12.6	35.0	11.2	7.0

tioned before, this property will always hold because of the monotonicity property of the Pareto curve. Finally, let us note that these intervals can still be incorporated into the formulation to make it tighter. Regarding this issue, it will be necessary to find the proper balance between a tighter formulation and an increase in the size of (P3).

- It may occur in some cases that the parametric NLP of the lower level will not be feasible in the entire interval $[\underline{\varepsilon}, \overline{\varepsilon}]$ for some vectors of binary variables. In these cases it will be necessary to introduce additional "artificial" intervals in the current best profile in order to be able to generate the entire Pareto set. These intervals will take a zero value and will cover the regions where the NLPs render infeasible.
- The integer cuts are added cumulatively at each iteration to the master MINLP, thus leading to an increase of its size.
- The proposed approach can also be applied to deterministic problems, where the life cycle inventory results per reference flow of activity are assumed to be known in advance. In this case, the problem can be posed as a parametric MILP and decomposed into a master MILP and a parametric LP, in a similar way as in the nonlinear case.
- The modeling framework and solution approach presented in this article can also handle the case in which the uncertain parameters are correlated (i.e., vary together). This requires the definition of the covariance matrix that describes the correlation between the uncertain parameters. Furthermore, the convexity property of the resulting MINLP still holds for this specific case.[45]

Case Studies

We next present two different examples that illustrate the application and computational effectiveness of the proposed algorithm. The models were implemented in GAMS 21.4[53] and solved with the MINLP solver DICOPT interacting with CPLEX 9.0 and SNOPT 6.2 on an Intel 1.2 GHz machine.

Case study 1

In this first example, we address the optimal retrofit of an existing SC established in Europe in terms of economic and environmental performance under uncertainty. The superstructure of the case study is depicted in Figure 8, whereas the set of available technologies is given in Figure 9. Specifically, there are 6 different technologies available to manufacture 6 main products. The original SC comprises 1 plant and 1 warehouse that are both placed in Tarragona (Spain), and 4 final markets that are located in the following European cities: Leuna (Germany), Neratovice (Czech Republic), Sines (Portugal) and Tarragona. The demand is expected to increase in Leuna and Neratovice, so the problem consists of determining whether it is better to expand the capacity of the existing plant or open a new one in Neratovice, which would be close to the growing markets.

A demand satisfaction target level of 85% must be attained in each of the years in which the total time horizon of 3 years is divided. The existing plant has an installed capacity of 100 kton/year for each available technology, whereas the capacity of the existing warehouse equals 100 kton. The lower and upper limits within which the capacity expansions must fall are 50 and 400 ktons/year for plants and 50 and 400 ktons for warehouses, respectively. No bounds on the total number of expansions of plants and warehouses are imposed. Furthermore, no upper limits on the purchases of raw materials are fixed. On the other hand, to prevent outsourcing from taking place, we set zero upper limits on purchases of intermediate and final products. The lower and upper bounds on the flows of materials between plants and warehouses and warehouses and markets are 5 and 500 kton/year in both cases, respectively. The turnover ratio is equal to 10 and the initial inventories at the warehouses are assumed to be zero. No minimum production levels are fixed at the plants. The interest rate, the salvage value and the tax rate are equal to 10%, 20% and 30%, respectively. This example assumes low unitary transportation costs equal to 0.4 ¢/ton·km. The fixed investment terms associated with the establishment of transportation links are all set to zero.

All the remaining data associated with the problem is given in Tables 1–7.

Table 6. Case Study 1: Matrix of Distances

	λ_{kl}^{WH} (km)			
Ware./Market	Leuna	Neratovice	Sines	Tarragona
Neratovice	295.45	0	2,970.72	1,855.47
Tarragona	1781.36	1855.47	1,212.82	0

Table 7. Case Study 1: Variable and Fixed Investment Costs and Inventory Costs Associated with Warehouses for $t = 1$ (assume a 5% increase in each period of time)

Warehouse	α_{kt}^{WH} (\$/ton)	β_{kt}^{WH} (thousand \$)	π_{kt} (\$/ ton·year)
Neratovice	1.98	180.58	0.18
Tarragona	2.38	216.69	0.22

Table 8. Case Study 1: Progress of Iterations

	Upper level		Lower level	Total time
Iteration	Intersection	Time (CPU s)	Time (CPU s)	(CPU s)
1	653.45	1.56	2.82	4.38
2	651.44	1.11	7.19	8.30
3	648.24	1.27	8.56	9.83
4	635.88	1.59	7.13	8.72
5	609.94	2.31	6.33	8.64
6	595.80	0.91	5.06	5.97
7	Infeasible	22.46	–	22.46
Total		**31.21**	**37.09**	**68.30**

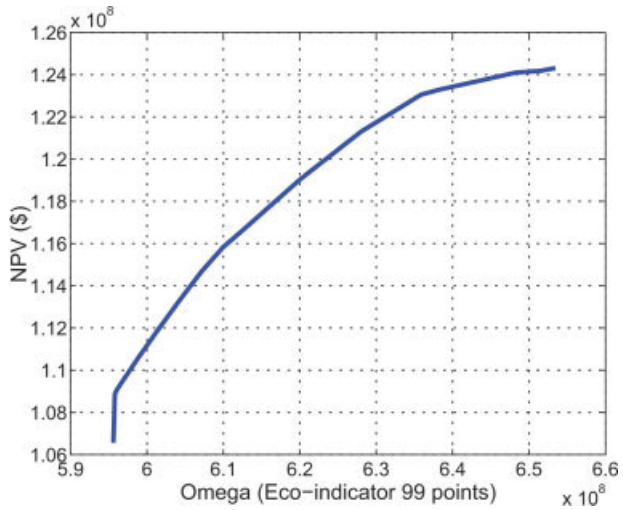

Figure 10. Pareto set of case study 1.

[Color figure can be viewed in the online issue, which is available at www.interscience.wiley.com.]

The sources of the emission inventories for the illustrative example have been taken from different databases that are integrated within the Simapro software.[37] The direct emissions associated with the manufacturing technologies are neglected. We assume standard deviations of 5, 10 and 20% for the entries of the life cycle inventories of the energy generation, raw materials production and transportation tasks, respectively. The probability level κ is set to 90%.

The values of $\underline{\varepsilon}$ and $\overline{\varepsilon}$ are first calculated by solving (P1a) and (P1b), respectively. Note that (P1b) can be reformulated as an MILP by dropping the nonlinear constraint that defines Ω. On the other hand, (P1a) takes the form of a convex MINLP. The solution of the aforementioned MILP provides the first point of the Pareto set. The vector of binary variables given by this solution is next fixed in the lower level,

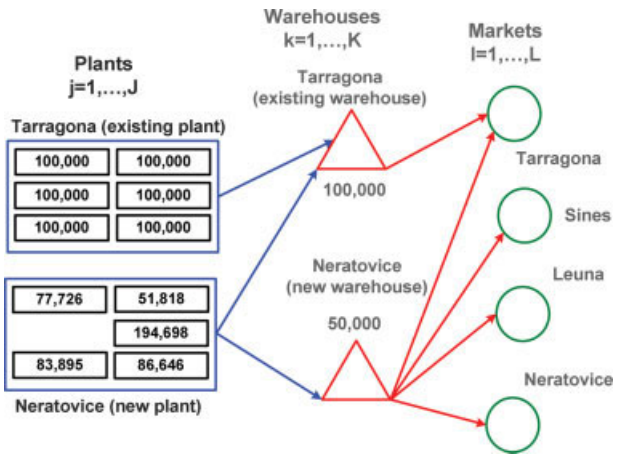

Figure 11. Maximum NPV solution.

[Color figure can be viewed in the online issue, which is available at www.interscience.wiley.com.]

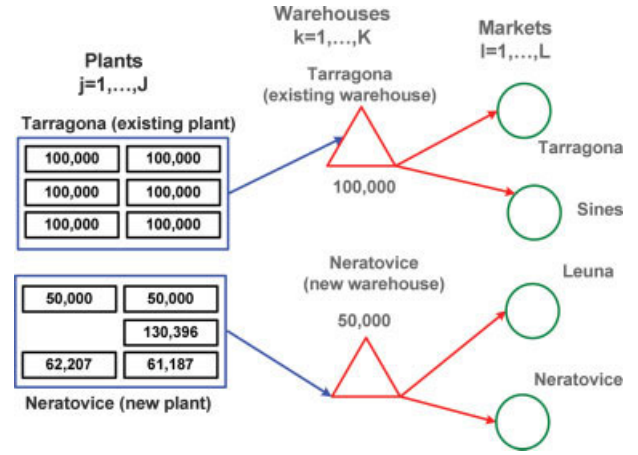

Figure 12. Minimum Ω solution.

[Color figure can be viewed in the online issue, which is available at www.interscience.wiley.com.]

and the associated parametric profile is determined. This profile is taken as a basis for future improvements. The algorithm then proceeds as described before until an infeasible MINLP is obtained in the upper level.

To initialize the parametric NLPs, we divide the original interval $[\underline{\varepsilon}, \overline{\varepsilon}]$ into 5 sub-intervals of equal length and solve the NLP for the limits of each of these sub-intervals. In each iteration the linearizations used to solve the parametric NLPs are added to the master MINLP in order to make it tighter, which in turn reduces the number of iterations required by DICOPT. The size of the master MINLP is kept constant by including only those linearizations corresponding to the last NLP being solved. The absolute optimality gap is set to $\$250{\cdot}10^3$ The tolerance error of the master problems is also fixed to $\$250{\cdot}10^3$. The single objective problem has 1,963 constraints, 1,837 continuous variables and 78 binary variables. Table 8 shows the solution times for the subproblems solved in each of the iterations of the proposed decomposition algorithm. The complete Pareto set is generated in 68.30 CPU seconds.

Figure 10 shows the Pareto curve obtained by following the proposed procedure. As can be observed, there is a clear trade-off between NPV and Ω, since reductions in the environmental impact can only be achieved by compromising the economic benefit of the SC. Each point of the Pareto set entails a specific SC structure and a set of planning decisions. In this context, the environmental impact under uncertainty is decreased by properly adjusting the design and planning variables according to the environmental requirements to be fulfilled in each case.

Figures 11 and 12 show the SC configurations of the extreme solutions. The figures in the plot represent the capacities of the plants and warehouses expressed in tons per year and tons, respectively. As can be observed, both solutions entail the construction of a new plant in Neratovice. However, they primarily differ in the SC topology and the total network capacity. In the maximum NPV solution, part of the total production is made in the new plant that will be opened in Neratovice, and then shipped to the warehouse that is close to the existing plant located in Tarragona. By

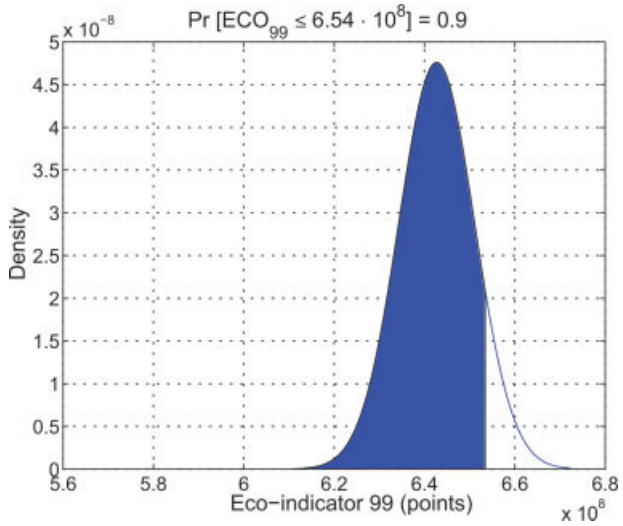

Figure 13. Probability curve of Eco-indicator 99 (maximum NPV solution).

[Color figure can be viewed in the online issue, which is available at www.interscience.wiley.com.]

doing so, the model takes advantage of the lower investment and production costs in Czech Republic compared with Spain. On the other hand, in the minimum Ω solution, products are manufactured as close as possible to the markets. This SC topology reduces the emissions due to the transportation tasks. The second difference lies in the SC capacity, which is lower in the minimum environmental impact design. In this solution, the production rates are reduced and the demand satisfaction level drops to its lower limit, which was set to 85%. Figures 13 and 14 depict the probability curves associated with the maximum NPV and minimum Ω solutions, respectively. As can be observed, when Ω is minimized, the probability curve is shifted to the left. This results in a reduction of the probability of high environmental impacts in the space of uncertain parameters.

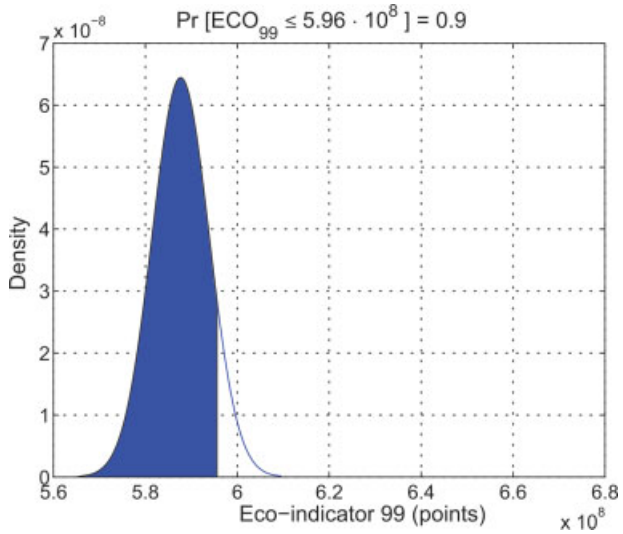

Figure 14. Probability curve of Eco-indicator 99 (minimum Ω solution).

[Color figure can be viewed in the online issue, which is available at www.interscience.wiley.com.]

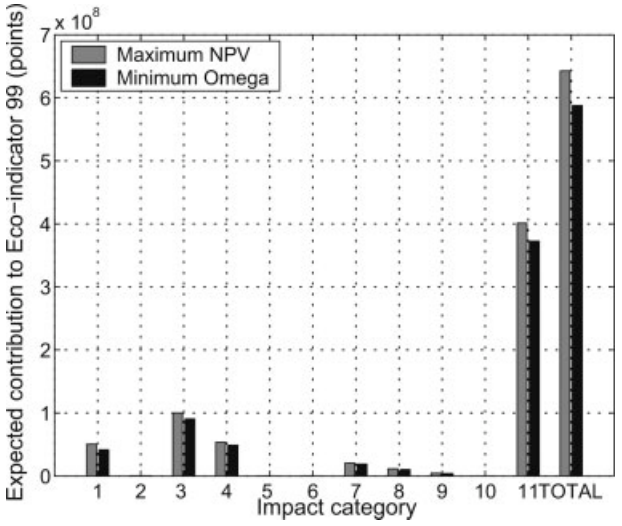

Figure 15. Impact categories of Eco-indicator 99.

Figure 15 depicts the expected value of the environmental impacts that are included in the Eco-indicator 99 for each of the extreme solutions. In both cases, the main impacts are: (1) carcinogenic effects on humans, (3) respiratory effects on humans caused by inorganic substances, (4) damage to human health caused by climate change, and (11) damage to resources caused by extraction of fossil fuels. Finally, Figures 16 and 17 show the contribution of the different sources of environmental damage to the total environmental impact. Note that in all the cases the generation of raw materials represents the most significant contribution to the total impact.

Case study 2

This second example addresses the optimal design of another SC to be established in Europe. There are three

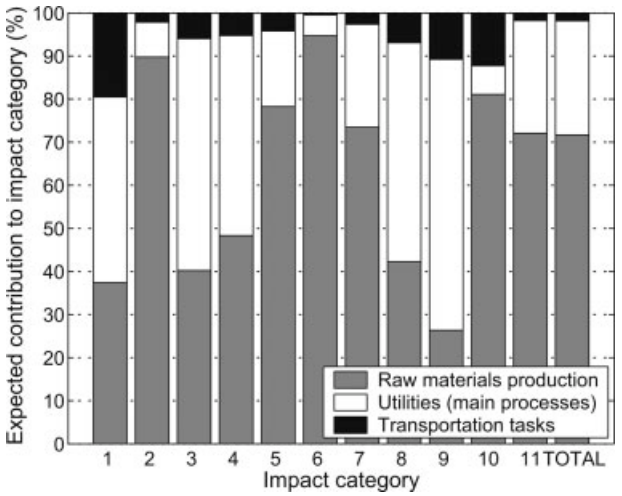

Figure 16. Expected contribution to Eco-indicator 99 (maximum NPV solution).

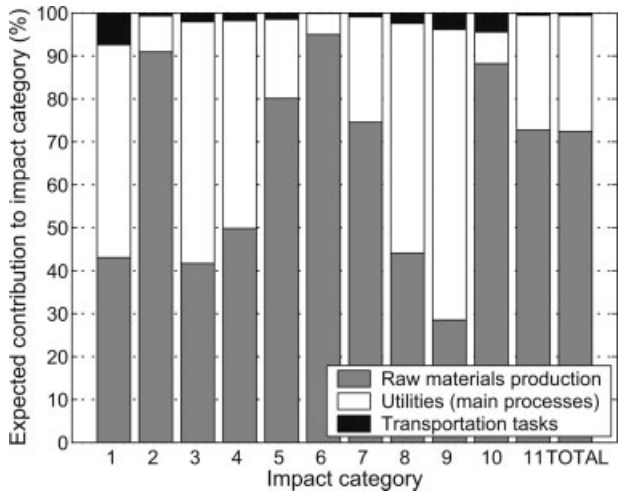

Figure 17. Expected contribution to Eco-indicator 99 (minimum Ω solution).

potential locations for plants and warehouses: Neratovice (Czech Republic), Tarragona (Spain) and Wloclaweck (Poland). The markets to be satisfied are located in Kazincbarcika (Hungary), Neratovice, Tarragona and Wloclaweck. The superstructure of the case study, which is given in Figure 18, comprises 20 different technologies that can manufacture 14 main products. Figure 19 depicts the main products associated with each technology, some of which can be recycled and used as raw materials in other processes.

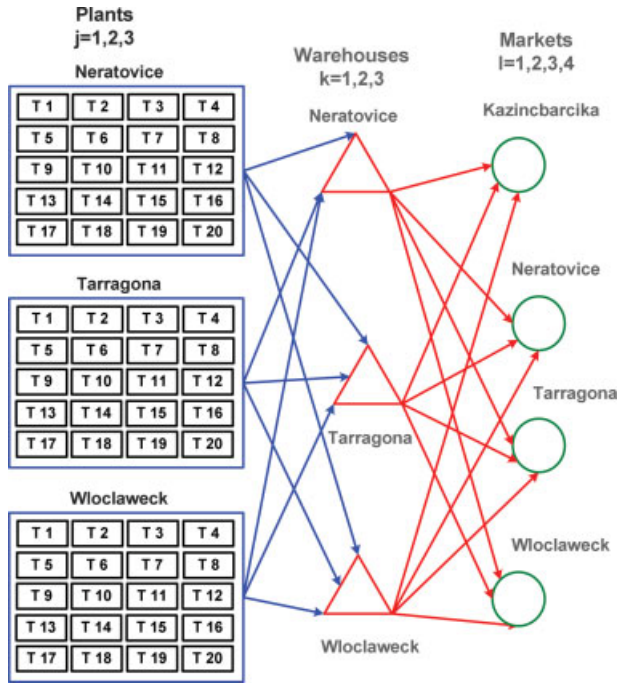

Figure 18. Case study 2.

[Color figure can be viewed in the online issue, which is available at www.interscience.wiley.com.]

The time horizon for this example is also 3 years. The minimum demand satisfaction level is 97.5%. No upper limits on the purchases of raw materials and intermediate products are imposed, whereas zero upper limits are set for final products. The lower and upper bounds on the flows of materials between plants and warehouses are 100 and 750 kton/year, respectively. The lower and upper bounds imposed to the capacity expansions are 7.5 and 500 ktons/year for plants and 10 and 500 ktons for warehouses. The mass balance coefficients associated with the different technologies have been take from the literature.[54] The lower and upper transport limits between warehouses and markets are 50 and 250 kton/year, respectively. The turnover ratio is equal to 10 and the initial inventories at the warehouses are assumed to be zero. No minimum production levels are fixed at the plants. The interest rate, the salvage value and the tax rate are equal to 10%, 20% and 30%, respectively. This example considers higher transportation costs (21 ¢/ton·km) than the previous one. Again, the fixed investment terms associated with the establishment of transportation links are all set to zero. All the remaining data associated with the problem is given in Tables 9–15.

The emission inventories for the generation of raw materials, intermediate products and utilities have also been taken from Simapro.[37] The direct emissions associated with the manufacturing technologies are neglected. We assume standard deviations of 15, 20 and 30% for the entries of the life cycle inventories of the energy generation, raw materials production and transportation tasks, respectively. The probability level κ is set to 90%.

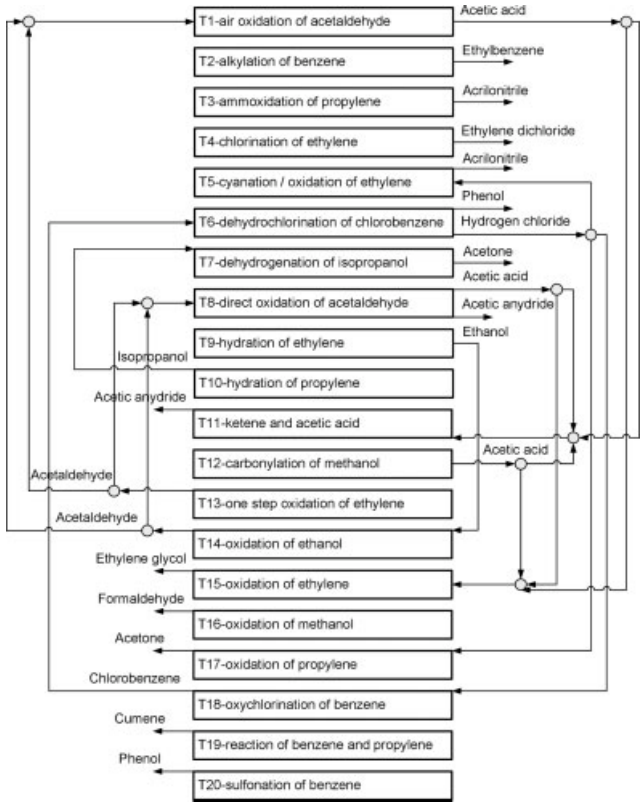

Figure 19. Superstructure of technologies of case study 2.

Table 9. Case Study 2: Variable and Fixed Investment Cost of Plants for $t = 1$ (assume a 5% increase in each period of time)

	α_{ijt}^{PL} ($ ·year/ton)			β_{ijt}^{PL} (thousand $)		
Tech./Plant	Neratovice	Tarragona	Wloclaweck	Neratovice	Tarragona	Wloclaweck
T1	87.31	128.05	104.77	7945.30	11653.11	9,534.36
T2	40.78	59.81	48.93	3711.00	5442.81	4,453.21
T3	235.81	345.85	282.97	21459.49	31473.91	25,751.38
T4	10.47	15.36	12.57	953.08	1397.85	1,143.70
T5	93.43	137.04	112.12	8502.82	12470.80	10,203.38
T6	140.24	205.68	168.28	12762.03	18717.64	15,314.43
T7	48.12	70.58	57.75	4379.21	6422.84	5,255.05
T8	166.68	244.46	200.01	15168.30	22246.84	18,201.96
T9	204.22	299.53	245.07	18585.07	27258.10	22,302.08
T10	104.73	153.60	125.68	9530.80	13978.51	11,436.97
T11	63.50	93.13	76.20	5778.40	8474.99	6,934.08
T12	87.31	128.05	104.77	7945.30	11653.11	9,534.36
T13	91.28	133.87	109.53	8306.45	12182.79	9,967.74
T14	67.46	98.95	80.96	6139.55	9004.67	7,367.46
T15	173.52	254.50	208.22	15790.94	23160.05	18,949.13
T16	68.84	100.97	82.61	6265.00	9188.66	7,517.99
T17	99.25	145.57	119.10	9032.12	13247.10	10,838.54
T18	33.15	48.63	39.79	3017.16	4425.17	3,620.59
T19	46.34	67.96	55.60	4216.72	6184.52	5,060.06
T20	129.03	189.25	154.84	11742.48	17222.31	14090.98

Table 10. Case Study 2: Operating Cost for $t = 1$ (assume a 5% increase in each period of time) and Consumption of Energy

	v_{ijpt} ($/ton)			η_{ijp}^{EN}
Tech./Plant	Neratovice	Tarragona	Wloclaweck	(FOET/ton)
T1	17.79	26.09	21.35	0.29
T2	1.40	2.06	1.68	0.02
T3	9.29	13.63	11.15	0.15
T4	6.26	9.18	7.51	0.10
T5	36.61	53.70	43.93	0.60
T6	32.36	47.46	38.83	0.53
T7	20.22	29.66	24.26	0.33
T8	19.61	28.77	23.54	0.32
T9	45.11	66.16	54.13	0.74
T10	23.26	34.11	27.91	0.38
T11	16.58	24.31	19.89	0.37
T12	13.54	19.86	16.25	0.27
T13	22.65	33.22	27.18	0.22
T14	13.54	19.86	16.25	0.22
T15	39.04	57.26	46.85	0.64
T16	0.19	0.28	0.23	0.00
T17	46.93	68.83	56.32	0.77
T18	12.33	18.08	14.79	0.20
T19	3.83	5.62	4.60	0.06
T20	12.94	18.97	15.52	0.21

Table 11. Case Study 2: Price of Final Products for $t = 1$ (assume a 5% increase in each period of time)

Chemical/	γ_{lpt}^{FP} ($/ton)			
Market	Kazincbarcika	Neratovice	Tarragona	Wloclaweck
Acetaldehyde	582.01	618.39	727.51	636.57
Acetic acid	564.37	599.65	705.47	617.28
Acetic anydride	881.83	936.95	1102.29	964.51
Acetone	511.46	543.43	639.33	559.41
Acrylonitrile	917.11	974.43	1146.38	1003.09
Chlorobenzene	917.11	974.43	1146.38	1003.09
Cumene	458.55	487.21	573.19	501.54
Ethanol	599.65	637.13	749.56	655.86
Ethylbenzene	458.55	487.21	573.19	501.54
Ethylene dichloride	352.73	374.78	440.92	385.80
Ethylene glycol	793.65	843.25	992.06	868.06
Formaldehyde	493.83	524.69	617.28	540.12
Isopropanol	458.55	487.21	573.19	501.54
phenol	811.29	861.99	1014.11	887.35

Table 12. Case Study 2: Cost of Raw Materials for $t = 1$ (assume a 5% increase in each period of time)

	γ_{jpt}^{RM} ($/ton)		
Chemical/Plant	Neratovice	Tarragona	Wloclaweck
Ammonia	124.01	181.88	148.81
Benzene	176.92	259.48	212.30
Carbon monoxide	41.34	60.63	49.60
Chlorine	99.21	145.50	119.05
Ethylene	206.18	302.40	247.42
Hydrogen chloride	102.51	150.35	123.02
Hydrogen cyanide	413.36	606.26	496.03
Methane	74.40	109.13	89.29
Methanol	115.74	169.75	138.89
Methyl acetate	99.21	145.50	119.05
Oleum	42.99	63.05	51.59
Oxygen	26.46	38.80	31.75
Propylene	140.54	206.13	168.65
Sodium hydroxide	33.07	48.50	39.68
Sodium sulfite	41.34	60.63	49.60
Sulfuric acid	37.20	54.56	44.64

Table 13. Case Study 2: Demand of Products for $t = 1$ (assume a 5% increase in each period of time)

	$\overline{D_{lpt}^{MK}}$ (tons)			
Chemical/Market	Kazincbarcika	Neratovice	Tarragona	Wloclaweck
Acetaldehyde	5,788	6,381	7,757	8,144
Acetic acid	4,631	5,105	6,205	6,516
Acetic anydride	9,261	10,210	12,411	13,031
Acetone	4,631	5,105	6,205	6,516
Acrylonitrile	9,261	10,210	12,411	13,031
Chlorobenzene	4,631	5,105	6,205	6,516
Cumene	4,631	5,105	6,205	6,516
Ethanol	5,788	6,381	7,757	8,144
Ethylbenzene	5,788	6,381	7,757	8,144
Ethylene dichloride	9,261	10,210	12,411	13,031
Ethylene glycol	5,788	6,381	7,757	8,144
Formaldehyde	5,788	6,381	7,757	8,144
Isopropanol	9,261	10,210	12,411	13,031
Phenol	5,788	6,381	7,757	8,144

Table 14. Case Study 2: Matrix of Distances

	λ_{kl}^{WH} (km)			
Ware./Market	Kazincbarcika	Neratovice	Tarragona	Wloclaweck
Neratovice	695.5	0	1,855.5	277.1
Tarragona	2385.8	1855.5	0	2110.4
Wloclaweck	644.2	277.1	2110.4	0

Table 15. Case Study 2: Variable and Fixed Investment Costs and Inventory Costs Associated with Warehouses for $t = 1$ (assume a 5% increase in each period of time)

Warehouse	α_{kt}^{WH} (\$/ton)	β_{kt}^{WH} (thousand \$)	π_{kt} (\$ /ton · year)
Neratovice	1.98	180.57	1.81
Tarragona	2.91	264.84	2.65
Wloclaweck	2.38	216.69	2.17

Table 16. Case Study 2: Progress of Iterations

	Upper Level		Lower Level	
Iteration	Intersection	Time (CPU s)	Time (CPU s)	Total Time (CPU s)
1	737.59	62.39	48.32	110.71
2	730.55	13.18	61.74	74.92
3	718.02	25.79	56.75	82.54
4	708.35	15.38	45.18	60.56
5	Infeasible	3.73	–	3.73
Total		**120.47**	**211.99**	**332.46**

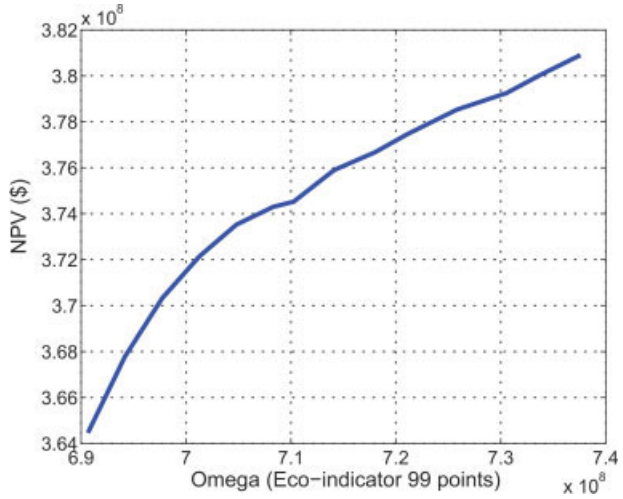

Figure 20. Pareto set of case study 2.

[Color figure can be viewed in the online issue, which is available at www.interscience.wiley.com.]

The problem is solved in a similar way as was done in the previous example. The parametric NLPs of the lower level are calculated with an absolute optimality gap of $\$500 \cdot 10^3$. The tolerance error of the master problems is also fixed to $\$500 \cdot 10^3$. This case study leads to a larger master MINLP, the solution of which is expedited by making use of a customized initialization scheme. Specifically, in each iteration the linearizations used to solve the parametric NLP of the lower level are employed to construct a linear outer approximation of the original master MINLP, in which the convex nonlinear equation that defines Ω is replaced by a set of linear inequality constraints. The resulting MILP, which is solved with CPLEX, provides an integer solution that is used

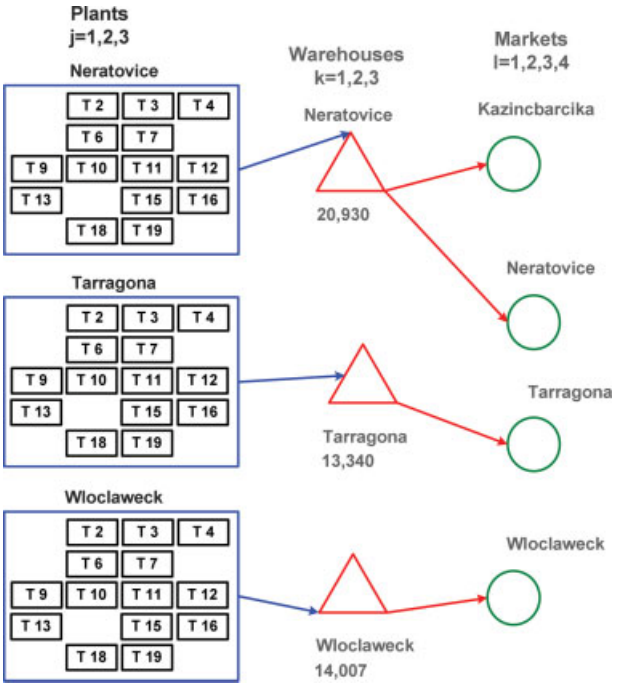

Figure 21. Maximum NPV solution.

[Color figure can be viewed in the online issue, which is available at www.interscience.wiley.com.]

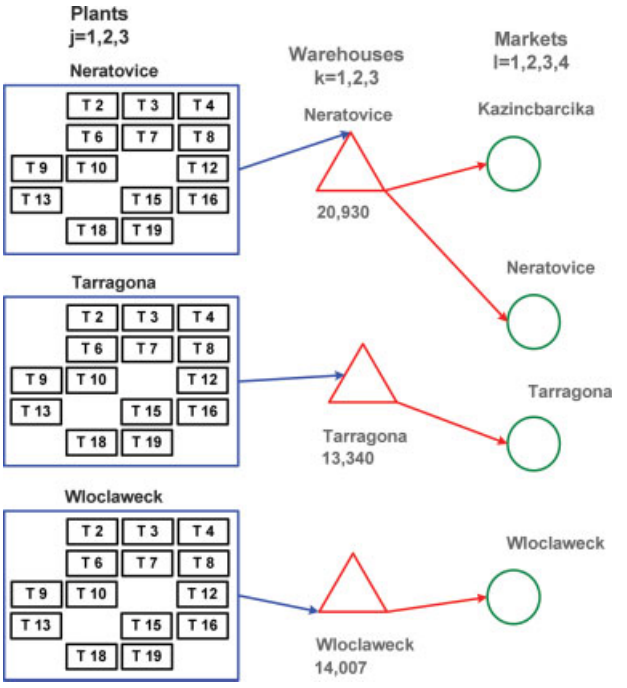

Figure 22. Minimum Ω solution.

[Color figure can be viewed in the online issue, which is available at www.interscience.wiley.com.]

Table 17. Case Study 2: Capacity of Technologies at Plants Expressed in tons/year

	Maximum NPV solution			Minimum Omega solution		
Tech./Plant	Neratovice	Tarragona	Wloclaweck	Neratovice	Tarragona	Wloclaweck
T1	–	–	–	–	–	–
T2	13,417	8,552	8,979	13,081	8,338	8,755
T3	20,956	13,357	14,025	20,432	13,023	13,684
T4	21,467	13,683	14,367	21,467	13,683	14,367
T5	–	–	–	–	–	–
T6	13,417	8,552	8,979	13,081	8,338	8,755
T7	10,478	7,500	7,500	10,216	7,500	7,500
T8	–	–	–	20,432	13,023	13,674
T9	13,097	8,348	8,765	12,770	8,240	8,546
T10	33,098	21,277	22,340	32,270	20,745	21,782
T11	20,956	13,357	14,025	–	–	–
T12	37,066	23,625	24,806	7,500	7,500	7,500
T13	13,417	8,552	8,979	35,148	22,403	23,523
T14	–	–	–	–	–	–
T15	13,097	8,348	8,765	12,770	8,338	8,546
T16	13,417	8,552	8,979	13,081	8,338	8,755
T17	–	–	–	–	–	–
T18	26,700	17,018	17,869	26,032	17,018	17,422
T19	10,734	7,500	7,500	10,734	7,500	7,500
T20	–	–	–	–	–	–

to bypass the first relaxed NLP solved by DICOPT. Thus, instead of solving a relaxed NLP, we solve an NLP where the binary variables are fixed. The starting point for this NLP is given by the solution of the aforementioned MILP. Furthermore, these linear inequalities (i.e., supporting hyperplanes) are added to the master MINLP in order to make it tighter, in a similar way as was done in the first example.

The single objective problem has 9,808 constraints, 10,231 continuous variables and 252 binary variables. Table 16 shows the solution times for the subproblems solved in each iteration of the algorithm. The complete Pareto set is generated in 332.46 CPU seconds.

Figure 20 depicts the Pareto curve associated with the problem, whereas Figures 21 and 22 show the SC configurations associated with each of the extreme solutions and the capacities of the warehouses expressed in tons. The capacities of the technologies installed at the plants are given in Table 17. As can be observed, both solutions entail the establishment of a plant and a warehouse in each potential location. Furthermore, the warehouses fulfill the demand of the nearest markets and avoid long-distance shipments of products. The reason why both solutions present similar topological features lies in the high transportation costs assumed in the example. Thus, given this data, the maximum NPV and minimum environmental solutions will both try to minimize the transportation distance between the SC nodes, since this will simultaneously result in lower costs and environmental impacts. On the other hand, the solutions differ in the tech-

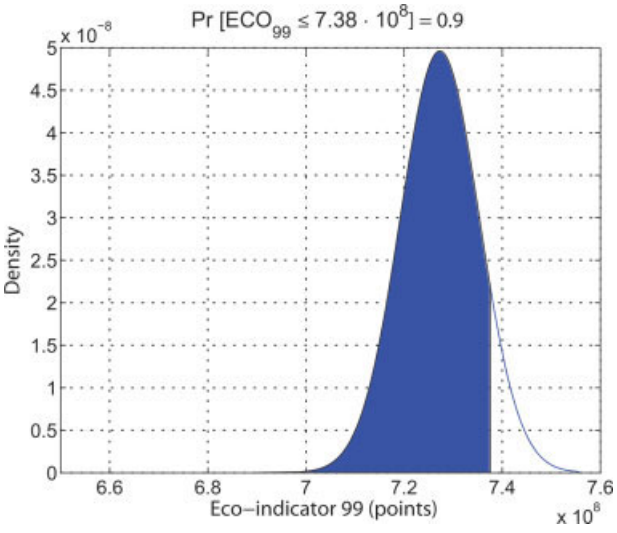

Figure 23. Probability curve of Eco-indicator 99 (maximum NPV solution).

[Color figure can be viewed in the online issue, which is available at www.interscience.wiley.com.]

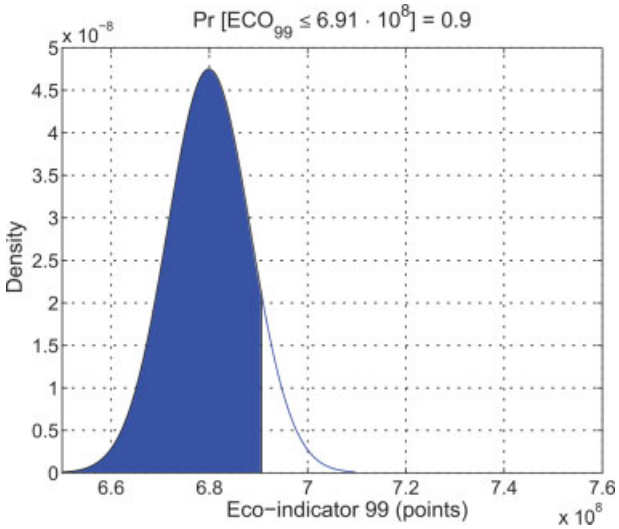

Figure 24. Probability curve of Eco-indicator 99 (minimum Ω solution).

[Color figure can be viewed in the online issue, which is available at www.interscience.wiley.com.]

nology selected for the production of acetic anhydride. The maximum NPV solution produces this chemical from ketene and acetic acid, which is the cheapest reaction pathway. On the other hand, the minimum Ω solution employs the oxidation of acetaldehyde, which leads to higher costs but causes less environmental impact. The second difference lies in the total production capacity of the SC, which is lower in the minimum environmental impact design.

Figures 23 and 24 depict the probability curves associated with the maximum NPV and minimum Ω solutions, respectively. As in the previous case, the probability curve is shifted to the left. This results in a reduction of the probability of high environmental impacts in the space of uncertain parameters.

Conclusions

This article has addressed the optimal design and planning of chemical processes under uncertainty in the life cycle inventory. The problem has been mathematically formulated as a bi-criterion stochastic MINLP that accounts for the maximization of the NPV and minimization of the environmental impact for a given probability level. The environmental performance has been measured through the Eco-indicator 99, which includes the recent advances made in LCA. The deterministic equivalent of such a model has been obtained by reformulating the chance constraint required to calculate the environmental performance in the space of uncertain parameters. The resulting deterministic bi-criterion MINLP has been further reformulated as a parametric MINLP, which has been solved by decomposing it into two problems and iterating between them.

The capabilities of our approach have been highlighted through two case studies. Numerical examples have shown that our modeling framework and solution strategy can be effectively used to control the variability of the environmental impact in the space of uncertain parameters. This goal is met by properly adjusting the design and planning SC decisions according to the environmental needs to be fulfilled in each case. The solutions obtained by our method provide valuable insights into the design problem and are intended to guide the decision-maker towards the adoption of more sustainable process alternatives.

Acknowledgments

Gonzalo Guillén-Gosálbez expresses his gratitude for the financial support received from the Fulbright/Spanish Ministry of Education and Science visiting scholar program. Gonzalo Guillén-Gosálbez also wishes to acknowledge support of this research work from the Spanish Ministry of Education and Science (Project No. DPI2008-04099/DPI) and the Spanish Ministry of External Affairs (Projects No. A/8502/07 and HS2007-0006).

Notation

Indices

b = environmental burdens
c = impact categories
d = damage categories
i = manufacturing technologies
j = plants
k = warehouses
l = markets
p = products
t = time periods

Sets

ID(d) = set of impacts c contributing to damage category d
IN(p) = set of manufacturing technologies that consume p
MP(i) = set of main products p of technology i
OUT(p) = set of manufacturing technologies that produce p

Parameters

$\overline{CE}_{ijt}^{PL}$ = upper bound on the capacity expansion of manufacturing technology i at plant j in time period t
$\underline{CE}_{ijt}^{PL}$ = lower bound on the capacity expansion of manufacturing technology i at plant j in time period t
$\overline{CE}_{kt}^{WH}$ = upper bound on the capacity expansion of warehouse k in time period t
$\underline{CE}_{kt}^{WH}$ = lower bound on the capacity expansion of warehouse k in time period t
$\overline{D}_{lpt}^{MK}$ = maximum demand of product p sold at market l in period t
$\underline{D}_{lpt}^{MK}$ = minimum demand of product p to be satisfied at market l in period t
ir = interest rate
$\overline{FCI}$ = upper limit on the total capital investment
$nexp_{ij}^{PL}$ = maximum number of capacity expansions for technology i available at plant j
$nexp_{k}^{WH}$ = maximum number of capacity expansions for warehouse k
NT = number of time periods
$\overline{PU}_{jpt}$ = upper bound on the purchases of product p at plant j in period t
$\underline{PU}_{jpt}$ = lower bound on the purchases of product p at plant j in period t
$\overline{Q}_{jkt}^{PL}$ = upper bound on the flow of materials between plant j and warehouse k in time period t
$\underline{Q}_{jkt}^{PL}$ = lower bound on the flow of materials between plant j and warehouse k in time period t
$\overline{Q}_{klt}^{WH}$ = upper bound on the flow of materials between warehouse k and market l in time period t
$\underline{Q}_{klt}^{WH}$ = lower bound on the flow of materials between warehouse k and market l in time period t
sv = salvage value
tor_k = turnover ratio of warehouse k
μ_{ip} = mass balance coefficient associated with product p and manufacturing technology i
φ = tax rate
γ_{lpt}^{FP} = price of final product p sold at market l in time period t
γ_{jpt}^{RM} = price of raw material p purchased at plant j in time period t
υ_{ijpt} = operating cost of manufacturing technology i available at plant j per unit of main product p in time period t
π_{kt} = inventory cost at warehouse k in period t
ψ_{jkpt}^{PL} = unitary transport cost of product p sent from plant j to warehouse k in time period t
ψ_{klpt}^{WH} = unitary transport cost of product p sent from warehouse k to market l in time period t
α_{ijt}^{PL} = variable investment term associated with technology i at plant j in time period t
β_{ijt}^{PL} = fixed investment term associated with technology i at plant j in time period t
α_{kt}^{WH} = variable investment term associated with warehouse k in time period t
β_{kt}^{WH} = fixed investment term associated with warehouse k in time period t
β_{jkt}^{TPL} = fixed investment term associated with the establishment of a transport link between plant j and warehouse k in time period t
β_{klt}^{TWH} = fixed investment term associated with the establishment of a transport link between warehouse k and market l in time period t
ω_{bp}^{PU} = emissions/feedstock requirements of chemical b per unit of raw material p generated
ω_{bp}^{PR} = emissions/feedstock requirements of chemical b per unit of intermediate/final product p generated

ω_b^{EN} = emissions/feedstock requirements of chemical b per unit of FOET combusted
ω_b^{TR} = emissions/feedstock requirements of chemical b per unit of mass transported one unit of distance
$\hat{\omega}_{bp}^{PU}$ = mean value of emissions/feedstock requirements of chemical b per unit of raw material p generated
$\hat{\omega}_{bp}^{PR}$ = mean value of emissions/feedstock requirements of chemical b per unit of intermediate/final product p generated
$\hat{\omega}_b^{EN}$ = mean value of emissions/feedstock requirements of chemical b per unit of FOET combusted
$\hat{\omega}_b^{TR}$ = mean value of emissions/feedstock requirements of chemical b per unit of mass transported one unit of distance
σ_{bp}^{PU} = standard deviation of emissions/feedstock requirements of chemical b
σ_{bp}^{PR} = standard deviation of emissions/feedstock requirements of chemical b per unit of raw material p generated
σ_p^{EN} = standard deviation of emissions/feedstock requirements of chemical b per unit of FOET combusted
σ_p^{TR} = standard deviation of emissions/feedstock requirements of chemical b per unit of mass transported one unit of distance
η_{ijp}^{EN} = energy consumed per unit of chemical p produced with manufacturing technology i at plant j
λ_{jk}^{PL} = distance between plant j and warehouse k
λ_{kl}^{WH} = distance between warehouse k and market l
θ_{bc} = damage factor of chemical b contributing to impact category c
κ = probability level (i.e., probability of yielding an Eco-indicator 99 value lower than Ω)
δ_d = normalization factor for damage category d
ξ_d = weighting factor for damage category d
τ = minimum desired percentage of the available installed capacity that must be utilized

Variables

C_{ijt}^{PL} = capacity of manufacturing technology i at plant j in time period t
CE_{ijt}^{PL} = capacity expansion of manufacturing technology i at plant j in time period t
C_{kt}^{WH} = capacity of warehouse k in time period t
CE_{kt}^{WH} = capacity expansion of warehouse k in time period t
CF_t = cash flow in period t
DAM_d = impact in damage category d
DEP_t = depreciation term in period t
ECO_{99} = Eco-indicator 99
$\hat{ECO}_{99}$ = mean value of the Eco-indicator 99
ECO_{99}^{SD} = standard deviation of the Eco-indicator 99
FCI = fixed capital investment
$FTDC_t$ = fraction of the total depreciable capital that must be paid in period t
IL_{kt} = average inventory level at warehouse k in time period t
IM_c = damage in impact category c
INV_{kpt} = inventory of product p kept at warehouse k in period t
LCI_b = life cycle inventory entry (i.e., emissions/feedstock requirements) associated with chemical b
NE_t = net earnings in period t
NPV = net present value
PU_{jpt} = purchases of product p made by plant j in period t
Q_{jkpt}^{PL} = flow of product p sent from plant j to warehouse k in period t
Q_{klpt}^{WH} = flow of product p sent from warehouse k to market l in period t
SA_{lpt} = sales of product p at market l in time period t
W_{ijpt} = input/output flow of product p associated with technology i at plant j in t
X_{ijt}^{PL} = binary variable (1 if the capacity of manufacturing technology i at plant j is expanded in time period t, 0 otherwise)
X_{kt}^{WH} = binary variable (1 if the capacity of warehouse k is expanded in time period t, 0 otherwise)
Y_{jkt}^{PL} = binary variable (1 if a transportation link between plant j and warehouse k is established in time period t, 0 otherwise)
Y_{klt}^{WH} = binary variable (1 if a transportation link between warehouse k and market l is established in time period t, 0 otherwise)
Ω = Eco-indicator 99 value for a probability level equal to κ

Literature Cited

1. Bok JW, Grossmann IE, Park S. Supply chain optimization in continuous flexible process networks. *Ind Eng Chem Res*. 2000;39:1279–1290.
2. Tsiakis P, Shah N, Pantelides CC. Design of multi-echelon supply chain networks under demand uncertainty. *Ind Eng Chem Res*. 2001;40:3585–3604.
3. Gupta A, Maranas CD. Managing demand uncertainty in supply chain planning. *Comput Chem Eng*. 2003;27:1219–1227.
4. Perea-López E, Ydstie E, Grossmann I. Managing demand uncertainty in supply chain planning. *Comput Chem Eng*. 2003;27:1201–1218.
5. van den Heever SA, Grossmann IE. A strategy for the integration of production planning and reactive scheduling in the optimization of a hydrogen supply network. *Comput Chem Eng*. 2003;27:1813–1839.
6. Grossmann IE. Enterprise-wide optimization: a new frontier in process systems engineering. *AIChE J*. 2005;51:1846–1857.
7. Guillén G, Espuña A, Puigjaner L. Addressing the scheduling of chemical supply chains under demand uncertainty. *AIChE J*. 2006;52:3864–3881.
8. Beamon BM. Supply chain design and analysis: models and methods. *Int J Production Econ*. 1998;55:281–294.
9. Lee HL, Billington C. Material management in decentralized supply chains. *Oper Res*. 1993;41:835–847.
10. You F, Grossmann IE. *Optimal Design and Operational Planning of Responsive Process Supply Chains*; book chapter in Process System Engineering: Volume 3: Supply Chain Optimization (Papageorgiou and Georgiadis, editors). Weinheim: Wiley-VCH, 2007:107–128.
11. Voudouris VT. Mathematical programming techniques to debottleneck the supply chain of fine chemicals. *Comput Chem Eng*. 1996;20S:S1296–S1274.
12. Georgiadis MC, Pistikopoulos EN. An integrated framework for robust and flexible process systems. *Ind Eng Chem Res*. 1999;38:133–143.
13. Aseeri A, Bagajewicz M. New measures and procedures to manage financial risk with applications to the planning of gas commercialization in Asia. *Comput Chem Eng*. 2004;28:2791–2821.
14. Guillén G, Mele F, Bagajewicz M, Espuña A, Puigjaner L. Multiobjective supply chain design under uncertainty. *Chem Eng Sci*. 2005;60:1535–1553.
15. Cano-Ruiz JA, McRae GJ. Environmentally conscious chemical process design. *Annu Rev Energy Environ*. 1998;23:499–536.
16. Srivastava SK. Green supply-chain management: a state-of-the-art literature review. *Int J Manag Rev*. 2007;9:53–80.
17. Zhou Z, Cheng S, Hua B. Supply chain optimization of continuous processes industries with sustainability considerations. *Comput Chem Eng*. 2000;24:1151–1158.
18. Al-Sharrah GK, Alatiqi I, Elkamel A, Alper E. Planning an integrated petrochemical industry with an environmental objective. *Ind Eng Chem Res*. 2001;40:2103–2111.
19. Lankey RL, Anastas PT. Life-cycle approaches for assessing green chemistry technologies. *Ind Eng Chem Res*. 2002;41:4498–4502.
20. Arena U, Mastellone ML, Perugini F, Clift R. Environmental assessment of paper waste management options by means of LCA methodology. *Ind Eng Chem Res*. 2004;43:5702–5714.
21. Hugo A, Pistikopoulos EN. Environmentally conscious long-range planning and design of supply chain networks. *J Cleaner Production*. 2005;13:1471–1491.
22. Stefanis SK, Livingston AG, Pistikopoulos EN. Environmental impact considerations in the optimal design and scheduling of batch processes. *Comput Chem Eng*. 1997;21:1073–1094.
23. Azapagic A, Clift R. The application of life cycle assessment to process optimisation. *Comput Chem Eng*. 1999;10:1509–1526.
24. Cabezas H, Bare JC, Mallick SK. Pollution prevention with chemical process simulators: the generalized waste reduction (WAR) algorithm - full version. *Comput Chem Eng*. 1999;23:623–634.
25. El-Halwagi MM, Gabriel F, Harell D. Rigorous graphical targeting for resource conservation via material recycle/reuse networks. *Ind Eng Chem Res*. 2003;42:4319–4328.
26. Bonfill A, Bagajewicz M, Espuña A, Puigjaner L. Risk management in scheduling of batch plants under uncertain market demand. *Ind Eng Chem Res*. 2004;43:741–750.
27. Gupta A, Maranas CD. A two-stage modelling and solution framework for multisite midterm planning under demand uncertainty. *Ind Eng Chem Res*. 2000;39:3799–3813.

28. Current J, Min H, Schilling D. Multiobjective analysis of facility location decisions, invited review. *Eur J Oper Res*. 1990;49:295–307.
29. Sahinidis NV, Grossmann IE, Fornari RE, Chathrathi M. Optimisation model for long range planning in the chemical industry. *Comput Chem Eng*. 1989;13:1049–1063.
30. Shapiro JF. *Modeling the Supply Chain*. Cambridge, MA: MIT Press, 2001.
31. PRé-Consultants, The Eco-indicator 99, A damage oriented method for life cycle impact assessment.Methodology Report and Manual for Designers. Technical Report, PRé Consultants, Amersfoort, The Netherlands, 2000.
32. Guinée JB, Gorrée M, Heijungs R, Huppes G, Kleijn R, de Koning A, van Oers L, Sleeswijk AW, S. Suh S, de Haes HAU, de Bruijn H, van Duin R, Huijbregts MAJ. *Handbook on Life Cycle Assessment. Operational Guide to the ISO Standards*. Dordrecht: Kluwer Academic Publishers, 2002.
33. Petrie BAGBJ, Romagnoli J. Process synthesis and optimisation tools for environmental design: methodology and structure. *Comput Chem Eng*. 2000;24:1195–1200.
34. Hoffmann VH, Hungerbuhler K, McRae GJ. Multiobjective screening and evaluation of chemical process technologies. *Ind Eng Chem Res*. 2001;40:4513–4524.
35. Chen H, Shonnard DR. Systematic framework for environmentally conscious chemical process design: Early and detailed design stages. *Ind Eng Chem Res*. 2004;43:535–552.
36. Ecobalance-UK, *TEAM and DEAM*. Ecobalance UK, The Ecobilan Group, Arundel, UK (www.ecobalance.com/uk_team.php), 1998.
37. PRé-Consultants, *SimaPro 6 LCA software*. The Netherlands (www.pre.nl/simapro/default.htm), 1998.
38. PIRA-International, *PEMS 4 Database*. PIRA International, Leatherhead, UK (www.pira.co.uk/pack/lca_software.htm), 1998.
39. Heijungs R, Frischknecht R. Representing statistical distributions for uncertain parameters in LCA. *Int J Life Cycle Assess*. 2005;10:248–254.
40. Heijungs R, Suh S, Kleijn R. Numerical approaches to life cycle interpretation. *Int J Life Cycle Assess*. 2005;10:103–112.
41. Sugiyama H, Fukushima Y, Hirao M, Hellweg S, Hungerbühler K. Using standard statistics to consider uncertainty in industry-based life cycle inventory databases. *Int J Life Cycle Assess*. 2005;10:339–405.
42. Charnes A, Cooper WW. Normal deviates and chance constraints. *J Am Stat Assoc*. 1962;52:134.
43. Petkov SB, Maranas CD. Multiperiod planning and scheduling of multipurpose batch plants under demand uncertainty. *Ind Eng Chem Res*. 1997;36:4864–4881.
44. Li P, Arellano-Garcia H, Wozny G. Chance constrained programming approach to process optimization under uncertainty. *Comput Chem Eng*. 2008;32:25–45.
45. Kataoka S. A stochastic programming model. *Econometrica*. 1963; 31:181–196.
46. Ehrgott M. *Multicriteria Optimization*. Berlin: Springer, 2000.
47. Dua V, Pistikopoulos E. Parametric optimization in process systems engineering: theory and algorithms. *Proc Indian Natn Sci Acad*. 2003; 69:429–444.
48. Pertsinidis A, Grossmann IE, McRaet GJ. Parametric optimization of MILP programs and a framework for the parametric optimization of MINLPs. *Comput Chem Eng*. 1998;22:S205–S212.
49. Fiacco AV. *Introduction to Sensitivity and Stability Analysis in Nonlinear Programming*. New York: Academic Press, 1983.
50. Dua V, Pistikopoulos EN. An algorithm for the solution of multiparametric mixed integer linear programming problems. *Ann Oper Res*. 2000;99:123–139.
51. Balas E. An algorithm for the solution of multiparametric mixed integer linear programming problems. *Oper Res Lett*. 1998;76:279–283.
52. Raman R, Grossmann IE. Relation between MILP modeling and logical inference for chemical process synthesis. *Comput Chem Eng*. 1993;17:909–915.
53. Brooke A, Kendrik D, Meeraus A, Raman R, Rosenthal RE. *GAMS—A User's Guide*. Washington: GAMS Development Corporation, 1998.
54. Rudd D, Fathi-Ashar D, Trevino A, Stadtherr M. *Petrochemical Technology Assessment*. New York: Wiley, 1981.

Appendix

This section describes the method used to solve the parametric NLPs of the lower level of our algorithm. The outline of the algorithm, which is based on the work of Fiacco,[49] is as follows (see Figure A1):

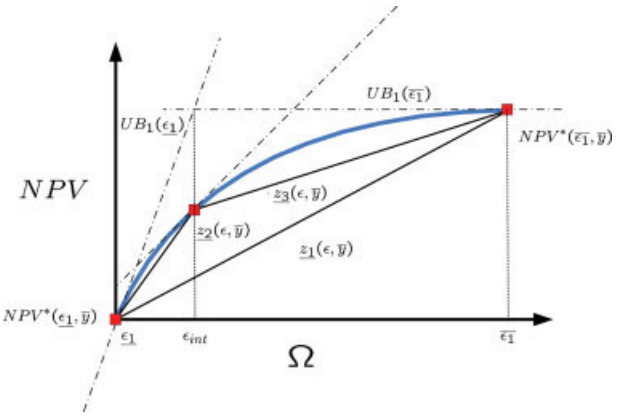

Figure A1. Parametric NLPs.

[Color figure can be viewed in the online issue, which is available at www.interscience.wiley.com.]

- **Step 1** (initialization). Set $n = 1$. Identify the lower and upper limits $\underline{\varepsilon_n}(\overline{y})$ and $\overline{\varepsilon_n}(\overline{y})$ of the environmental impact attained by the integer solution $\overline{y}$ provided by (P3).
- **Step 2**. Solve (P2) at the extreme points of the interval $[\underline{\varepsilon_n}(\overline{y}), \overline{\varepsilon_n}(\overline{y})]$. Let $\mathrm{NPV}^*(\underline{\varepsilon_n}, \overline{y})$ and $NPV^*(\overline{\varepsilon_n}, \overline{y})$ denote the optimal values of the objective function in each case.
- **Step 3** (parametric lower bound). Obtain a parametric lower bound $\underline{z_n}(\varepsilon, \overline{y})$ to the solution of (P2) in $[\underline{\varepsilon_n}(\overline{y}), \overline{\varepsilon_n}(\overline{y})]$. This step relies on the concavity property of the parametric solution of (P2). This property holds for nonlinear maximization problems with convex parametric constraints in the space of the continuous variables as well as the uncertain parameters, which turns out to be our case. It can be shown that under the concavity assumption, the connecting line segment:

$$\underline{z_n}(\varepsilon, \overline{y}) = \alpha \mathrm{NPV}^*(\underline{\varepsilon_n}, \overline{y}) + (1-\alpha)\mathrm{NPV}^*(\overline{\varepsilon_n}, \overline{y}) \quad \alpha \in (0,1) \tag{A1}$$

is a valid parametric lower bound of (P2) in the interval $[\underline{\varepsilon_n}(\overline{y}), \overline{\varepsilon_n}(\overline{y})]$.

- **Step 4** (parametric upper bound). A parametric upper bound of (P2) is given by:

$$\overline{z_n}(\varepsilon, \overline{y}) = \max\left(\mathrm{UB}_n(\underline{\varepsilon_n}), \mathrm{UB}_n(\overline{\varepsilon_n})\right) \tag{A2}$$

where $\mathrm{UB}_n(\underline{\varepsilon_n})$ and $UB_n(\overline{\varepsilon_n})$ are computed as follows:

$$\mathrm{UB}_n(\underline{\varepsilon_n}) = \mathrm{NPV}^*(\underline{\varepsilon_n}, \overline{y}) + \lambda_\varepsilon \mathrm{NPV}^*(\underline{\varepsilon_n}, \overline{y})(\varepsilon - \underline{\varepsilon_n}) \tag{A3}$$

$$UB_n(\overline{\varepsilon_n}) = NPV^*(\overline{\varepsilon_n}, \overline{y}) + \lambda_\varepsilon NPV^*(\overline{\varepsilon_n}, \overline{y})(\varepsilon - \overline{\varepsilon_n}) \tag{A4}$$

Here λ represent the Lagrangean multiplier associated with the parametric constraint. Notice that the validity of these bounds also relies on the concavity property of the parametric solution of (P2).

- **Step 5** (check convergence criteria). If the difference between the upper and lower bounds is within a given tolerance error then stop. Otherwise, increase the number of intervals by one $n = n + 1$ and sharpen the current upper and lower bounds by identifying the point where this difference

takes its maximum value. This point will lie in the intersection of two adjacent linear intervals of the current upper bound (i.e., $UB_n(\underline{\varepsilon_n})$ and $UB_n(\overline{\varepsilon_n})$). Let ε_{int} represent this point. Define the subintervals $[\underline{\varepsilon_n}(\overline{y}), \overline{\varepsilon_n}(\overline{y})]$ and $[\underline{\varepsilon_{n+1}}(\overline{y}), \overline{\varepsilon_{n+1}}(\overline{y})]$, where $\underline{\varepsilon_n}(\overline{y})$ and $\overline{\varepsilon_{n+1}}(\overline{y})$ are the lower and upper limits of the original interval, respectively, and $\overline{\varepsilon_n}(\overline{y}) = \underline{\varepsilon_{n+1}}(\overline{y}) = \varepsilon_{int}$. Go to step 2 and repeat steps 2 to 4 for all the subintervals generated so far until for a given number of intervals N the finalization criteria is met:

$$\overline{z_n}(\varepsilon, \overline{y}) - \underline{z_n}(\varepsilon, \overline{y}) \leq \text{tol} \quad n = 1, \ldots, N \tag{A5}$$

The following points of the algorithm should be highlighted:

- The parametric solution of (P2) $\widehat{z}(\varepsilon, \overline{y})$ is approximated by the lower bound LB_n in the final iteration (i.e., the current lower bound when the finalization criteria is met). Then, we have:

$$\widehat{z_n}(\varepsilon, \overline{y}) = \underline{z_n}(\varepsilon, \overline{y}) \quad n = 1, \ldots, N \tag{A6}$$

- The algorithm provides $n + 1$ solutions that can be used to construct a linear outer approximation of the convex feasible region of (P3). This linear outer approximation can then be added to the master problem in order to expedite its solution, which can be obtained via any suitable algorithm for MINLP. Thus, the optimal values x_n^* of the decision variables of (P2) that have been calculated in the N iterations of the parametric algorithm are used to obtain the following linear inequalities:

$$\Omega(x_n^*, \overline{y}) + \lambda_x \Omega(x_n^*, \overline{y})(x - x_n^*) \leq \varepsilon \quad n = 1, \ldots, N \tag{A7}$$

Due to the convexity property of $\Omega(x, \overline{y})$, these linear inequalities strictly underestimate the value of Ω and thus do not chop off any feasible solution when are added to (P3).

- The parametric algorithm can be expedited by making use of several starting points in the initialization step. Thus, at the initial phase, several NLPs are calculated for different points of the interval $[\underline{\varepsilon}, \overline{\varepsilon}]$. A possible way to generate these points consists of dividing the original interval into sub-intervals of equal length and then pick the lower and upper limits of each of them.

Manuscript received Apr. 23, 2008, and revision received Aug. 15, 2008.